CRANFIELD UNIVERSITY

DEVA NANDAN AJIT RAM

DEVELOPMENT OF HIGH-PERFORMANCE THERMAL SHIELDING FOR SPACE TRAVEL

SCHOOL OF AEROSPACE, TRANSPORT AND MANUFACTURING
MANUFACTURING

MASTERS OF SCIENCE BY RESEARCH(MSc-R)
Academic Year: 2021 - 2022

Supervisor: Prof. Krzysztof Koziol
Associate Supervisor: Dr.Alex Skordos
November 2022

CRANFIELD UNIVERSITY

SCHOOL OF AEROSPACE, TRANSPORT AND MANUFACTURING
MANUFACTURING

MASTERS OF SCIENCE BY RESEARCH(MSc-R)

Academic Year 2021- 2022

DEVA NANDAN AJIT RAM

DEVELOPMENT OF HIGH-PERFORMANCE THERMAL SHIELDING FOR SPACE TRAVEL

Supervisor: Prof. Krzysztof Koziol
Associate Supervisor: Dr.Alex Skordos
November 2022

This thesis is submitted in partial fulfilment of the requirements for the degree of Master of Science by Research
(NB. This section can be removed if the award of the degree is based solely on examination of the thesis)
© Cranfield University 2022. All rights reserved. No part of this publication may be reproduced without the written permission of the copyright owner.

ABSTRACT

Aerogel is a fascinating material system with uniquely high porous structure, consisting of 99.8% air, leading to properties with low density, high surface area and low thermal conductivity. They have been used in numerous application such as laser experiments, sensors (ultrasonic and gas), nuclear particle detection, thermal insulation, waste management, high explosive research and X-ray research. This thesis is focusing on the development of thermal insulation using aerogel suitable for use in extreme environments, the evaluation of material is obtained from the modelling dataset. Using the material properties from the literature a 3D composite slab model is created using SOLIDWORKS and is been analysed using ANSYS with environmental conditions. Numerous studies have been accomplished with the coating preparation of aerogel and its application on different materials. In this thesis, the material has been selected as a carbon-fibre slab and the coating is done using aerogel supported with various binders. Finally, from this thesis, a superlative binder is been found and discussed in the results. The report demonstrates the novel technique to coat aerogel on top of a composite without losing its properties and offering a way towards rapid manufacture of these advanced structures.

Keywords:

Aerogel, Carbon Fibre, Thermal insulation, 3D Modelling, ANSYS Analysis

ACKNOWLEDGEMENTS

Words cannot express my indebtedness to my supervisors, Prof. Krzysztof Koziol and Dr Alex Skordos for their invaluable support, forbearance and feedback throughout my thesis research. Their immense knowledge and plentiful experience have uplifted me during this research and daily life. I would like to thank Dr David Ayre, Dr Pavan Addepalli and Mr. Jim Hurley for their advice and technical support to my research. I would like to express my sincere thanks to all the members of Cranfield University for their help and support that have made my research and life in the UK wonderful time.

Finally, I must express my very profound gratitude to my parents and to my friends for providing me with unfailing support and continuous encouragement throughout my years of research and through the process of researching and writing this thesis. This accomplishment would not have been possible without them. Thank you.

TABLE OF CONTENTS

ABSTRACT iii
ACKNOWLEDGEMENTS iv
LIST OF FIGURES vii
LIST OF TABLES ix
LIST OF EQUATIONS x
1 Introduction 11
1.1 Current State of Art Technologies Of TPS 13
1.2 Challenges and Benefits of TPS 15
1.3 Aim and Objectives 16
2 Literature Review 17
2.1 Thermal Control Systems on Spacecraft 17
2.2 Current Insulation Technologies on Spacecrafts 18
2.3 Materials and Properties 21
2.4 State of Art Coating Techniques 28
2.5 Various Methods of Thermal Evaluations 29
2.6 Research Gap 30
3 Methodology 32
3.1 Theoretical Calculation 33
3.2 Modelling and Analysis 35
3.2.1 3D Modelling 35
3.2.2 Thermal and Mechanical Analysis 37
3.3 Solver Results 40
3.3.1 Modelling Results 40
3.3.2 Comparative Image from Solver Results 42
3.4 Laboratory Experimental Methods 44
3.4.1 Experimental setup 44
3.4.2 Design of Experiment 46
3.4.3 Experimental Preparations 47
3.4.4 Burn Testing 51
4 Results 53
4.1 Thermal Image (Lab Experimental Methods) 53
4.2 Comparative Results from Thermal Testing (Lab Experimental Methods) 56
4.3 Results of Burn Test (Lab Experimental Methods) 57
5 Discussion 59
6 Conclusion And Future Work 64
6.1 Conclusion 64
6.2 Future Work 65
REFERENCES 66
APPENDICES 70

Appendix A 70

LIST OF FIGURES

FIGURE 1 CLASSIFICATION OF TP 12
FIGURE 2 SCHEMATIC REPRESENTATION OF MODEL 33
FIGURE 3 3D SLAB MODEL USING SOLID WORKS 37
FIGURE 4 IMAGE OF MESHING IN ANSYS 39
FIGURE 5 IMAGE OF TEMPERATURE ANALYSIS 39
FIGURE 6 STEADY STATE THERMAL ANALYSIS 41
FIGURE 7 TOTAL DEFORMATION OF AEROGEL COATING 41
FIGURE 8 COMPARISON OF MAXIMUM SHEAR STRESS 42
FIGURE 9 COMPARISON OF TOTAL DEFORMATION 43
FIGURE 10 SCHEMATIC PRESTATION OF THE SETUP 44
FIGURE 11 ACTUAL SETUP 44
FIGURE 12 3D PRINTING OF FRAME 47
FIGURE 13 FRAME WITH SAMPLE 47
FIGURE 14 3D MODEL OF COMPOSITE WITH COATING 48
FIGURE 15 AEROGEL COATING ON COMPOSITE LAMINATE 49
FIGURE 16 GLASS BUBBLE COATING ON COMPOSITE LAMINATE 49
FIGURE 17 AEROGEL AND GLASS BUBBLE BLEND COATING ON COMPOSITE LAMINATE 50
FIGURE 18 SCHEMATIC REPRESENTATION OF BURN TEST 51
FIGURE 19 THERMAL IMAGE OF COMPOSITE AND COATING 54
FIGURE 20 THERMAL IMAGE OF COMPOSITE @ 60C 54
FIGURE 21 THERMAL IMAGE OF GLASS BUBBLE AND AEROGEL BLEND COATING 55
FIGURE 22 THERMAL IMAGE OF GLASS BUBBLE COATING 55
FIGURE 23 THERMAL IMAGE OF AEROGEL COATING 55
FIGURE 24 COMPARISON GRAPH OF AEROGEL AND GLASS BUBBLE 56
FIGURE 25 IMAGE OF COMPOSITE LAMINATE WITH AEROGEL COATING AFTER BURN TEST 58
FIGURE 26 IMAGE OF COMPOSITE LAMINATE WITH AEROGEL AND GLASS BUBBLE BLEND AFTER BURN TEST 58

FIGURE 27 COMPARISON OF THERMAL CONDUCTIVITY WITH AEROGEL PERCENTAGE 62

LIST OF TABLES

TABLE 1 CURRENT STATE OF ART TECHNOLOGIES 15
TABLE 2 PROPERTIES OF CARBON COMPOSITE 22
TABLE 3 PROPERTIES OF EPOXY LAMINATE 23
TABLE 4 PROPERTIES OF GLASS BUBBLES 25
TABLE 5 PROPERTIES OF AEROGEL 28
TABLE 6 PARAMETER FOR SOLVER 38
TABLE 7 THERMAL CAMERA SPECIFICATIONS 46
TABLE 8 PERCENTAGE DECREASE OF TEMPERATURE 59

LIST OF EQUATIONS

EQUATION 1 34
EQUATION 2 34
EQUATION 3 34
EQUATION 4 34
EQUATION 5 34
EQUATION 6 35

1 Introduction

The purpose of this research is to provide an overview of how to develop high-performance thermal insulation for spacecraft. Thermal protection systems (TPS) are used to shield spacecraft from the tremendous heat of atmospheric entry and re-entry. The requirement to guarantee the safety of payloads (people and cargo) has led to an increased international emphasis on the design and development of TPS as interplanetary missions gain popularity(Congdon et al., 2010)(Nenarokomov et al., 2016; Uyanna & Najafi, 2020). TPS is also used to protect solar probes from harm by keeping the spacecraft's exterior from heating up to dangerous levels as a consequence of the sun's powerful radiation. The TPS is not only an aerodynamic body and a structural part but also a thermal barrier that protects the payload from damage. From the earliest days of space travel, the consequences of excessive heating have been a deterrent to the pursuit of controlled hypersonic flight, prompting the development of fundamental TPS(del Val et al., 2022; Reynolds et al., 2013). Due to chemical reactions and gas dynamics processes that are still the topic of numerous ongoing studies, TPS design and material selection are challenging due to the mix of convective and radiative heat transfer mechanisms on the surface of the vehicle. So, it is crucial to pick materials for a vehicle's TPS based on a deep knowledge of these heat transfer processes via modelling, computational approaches, and tests. Therefore, a good TPS layout should protect the vehicle effectively from aerothermal stresses without adding too much weight or compromising its structural integrity (Congdon et al., 2010).

In the late 1920s, after studying the behaviour of space debris impacting with Earth's atmosphere, Robert Goddard, the creator of several critical automotive parts, proposed the use of an outer layer as a heat shield. Tsiolkovskiy, a rocketry and space travel pioneer, and Oberth, who worked on the idea at the same time reusable spacecraft were becoming famous, wrote about it(del Val et al., 2022). Oberth has previously concentrated on rocket systems' thrust efficiency. The Goddard decade soon after World War II represented the beginning of a golden age in space travel, with several nations trying to construct long-range missiles

and rockets that could escape Earth's atmosphere and then re-enter it to deliver specified payloads. The 1944 Oberth-Von Braun V-2 rocket engine was the first to pass the Karman line. Rockets became essential to human space flight after the V-2's success and the decision to pursue space exploration. Around this time, scientists undertook a number of experiments, but it quickly became evident that the vehicles and missiles being employed were incapable of reentering Earth's atmosphere at their planned velocities and temperatures because of their high heating and re-entry speeds(del Val et al., 2022).

This re-entry procedure resulted in hypersonic speeds and pressure spikes that were 25 times higher than atmospheric pressure. Moreover, several shock waves occurred because of the shock layer, and there was a lot of turbulence in the car because of the many flow field instabilities. The shock-wave interactions, in conjunction with the substantial thickening of the thermal boundary, caused a rise in temperature once the layer was transporting the energy to the vehicle's exterior. In addition to convective activity, these circumstances were notably prominent in the upper atmosphere, increasing the importance of radiant heating(del Val et al., 2022; Dombrovsky et al., 2017). Considering the structural TPS, it may utilize three different approaches, all of which attempt to keep materials at a constant temperature. Figure 1: 1) passive approaches, 2) active approaches, and 3) semi-passive approaches. A brief overview of these approaches is provided. There are a number of considerations when deciding on a TPS. Factors such as the heat flux, shape, and propulsion system depend on the surface and the length of time the light is falling on it(Gogu et al., 2009; Nguyen et al., 2019; J. Zhang et al., 2020).

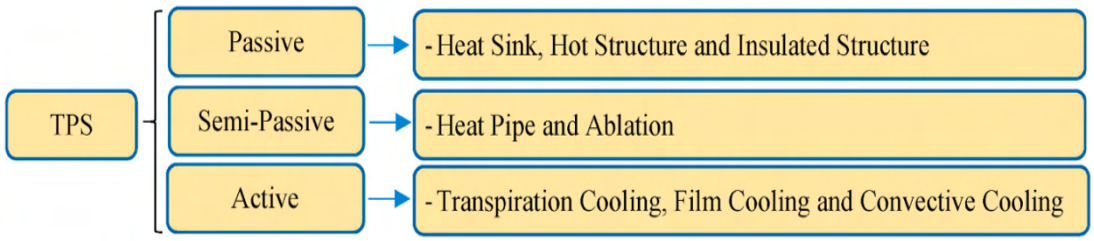

Figure 1 Classification of TP

1.1 Current State of Art Technologies Of TPS

Thermal protection systems keep the spacecraft's component systems at acceptable temperatures during the mission. The spacecraft must cope with extreme cold in deep space's shadows and searing heat in outer space's unfiltered direct sunlight. Spacecraft operation generates interior heat, which a TPS must manage. The spacecraft's inherent infrared radiation or an external coil can release heat from a TPS(Miao et al., 2021; Nenarokomov et al., 2016; J. Zhang et al., 2020). Thermal regulation is crucial to mission accomplishment because high or low temperatures can damage or impair components. To maximise performance, optical sensors, atomic clocks, and other components must be kept within a certain temperature stability range. Passive thermal protection systems technique includes eight types Table 1(del Val et al., 2022; Gogu et al., 2009):

Load-responsive insulation: One insulation system must respond to heat loads from launch (one atmosphere), ascent, and orbit (vacuum). Spray-on foam insulation optimises pre-launch and ascent but adds dead mass in orbit. Expanding multi-layer insulation (MLI) concepts thus the outer layer can withstand a gentle vacuum on Earth and compress somewhat while supported by a sophisticated spacer system is possible(Barrios & Van Sciver, 2010; Brindza et al., 2010; Dye et al., 2010).

Wrapped Insulation: Create space-worthy cryogen plumbing and component insulation. The idea is to wrap plumbing and components with MLI, but long-duration missions require innovative heat transfer methods below 0.25 W/m (Barrios & Van Sciver, 2010; Brindza et al., 2010; Dye et al., 2010).

Insulation with MMOD Protection: Novel MLI concepts reduce the necessity for low-conductivity paper between radiation shields. MMOD(Micrometeoroid and Orbital Debris) protection requires MLI system evaluation and enhancement. Self-healing materials that repair handling or micrometeoroids while preserving

thermal performance should be studied. Self-healing systems maybe 15–20 years away (Barrios & Van Sciver, 2010; Brindza et al., 2010; Dye et al., 2010).

Cooled Insulation Reduces and Eliminates Boil-Off: Large-scale insulation for broad-area coolers or hydrogen (H2) vapour-cooled shields for huge-diameter tanks is needed (Barrios & Van Sciver, 2010; Brindza et al., 2010; Dye et al., 2010).

Modelling Multi-layer Insulation: 1974 empirical formulae forecast multi-layer insulation heat loss. Heat loss per unit area is 2.5–5 times less accurate (Barrios & Van Sciver, 2010; Brindza et al., 2010; Dye et al., 2010).

Thermodynamics Structural Supports: Conduction heat loss from struts, skirts and feedlines can exceed convection and radiation heat loss from the tank surface. This loss needs innovative solutions. Actively cooling or vapour cooling these solid structures can improve conduction heat loss intercept at higher temperatures. A structure that disconnects from the load path on orbit is the best long-term answer. Cryogenic depot architecture requires autonomous docking cryogenic connections (Barrios & Van Sciver, 2010; Brindza et al., 2010; Dye et al., 2010).

Low-Temperature Radiators: Because they reject heat at low temperatures, they need huge surfaces. For very tiny weights in low-Earth orbit (LEO), the low-temperature limit is 50 Kelvin (K) (milliwatt scale). Deployable systems are needed for launch and orbital deployment with a wider radiative area. Launch materials should be flexible but rigid in space with strong emissivity. Cryogenic heat pipes and heat spreaders are needed. Scientific instruments need sub-4 K devices. Helium, hydrogen, and neon heat pipes can cool at 4 K, 15 K, and 40 K, respectively, since most fluids freeze at these temperatures. Fundamental material qualities prevent working fluids for 10 K two-phase circuits. Helium works below 6 K, hydrogen above 14 K, and no fluids in between. The TA 8 technological roadmap addresses cryogenic heat pipes (Barrios & Van Sciver, 2010; Brindza et al., 2010; Dye et al., 2010).

Table 1 Current State of Art Technologies(Dye et al., 2010)

Technology Name	Description
Load-Responsive Insulation	Multi-environment thermal insulation for spacecraft cryogenic propellant tanks
Wrapped Insulation	Thermal insulation for cryogenic tubing.
Insulation with Micrometeoroid and Orbital Debris	Protection Spacecraft cryogenic propellant-tank thermal insulation with micrometeoroid and orbital debris protection.
Cooled Insulation for Reduced and Zero Boil-off	Insulation integrated with broad area cooling (BAC) shields or hydrogen vapor-cooled shields.
Modelling for Multi-Layer	Insulation Empirical equations for low-temperature multi-layer insulation.
Low Thermal Conductivity Structural Supports	Structural supports for cryogenic propellant tanks that have low heat loss.
Low-Temperature Radiators	Spacecraft radiators that have high heat rejection at very low temperatures.
Cryogenic Heat Pipes	Heat pipes and heat spreaders that are effective at temperatures below 50 K. Specialized applications require devices that operate below 4 K.

1.2 Challenges and Benefits of TPS

The current passive thermal control technologies need improvement. Modern multilayer insulation (MLI) concepts increase mass and reduce performance by spacing radiation layers with low thermal conductivity paper. MLI with MMOD

protection and ground-to-flight insulation has not been proven(Miao et al., 2022; Natali et al., 2016). The goal is to maximize passive cooling or insulation with acceptable structural qualities and the lowest system mass. Many of these technologies will be driven by material development and should include dual functionality like micrometeorite protection. Insulation for mission stages, low-conductivity structures and supports, radiators, and heat pipes are in this category. Lower mass and higher performance are projected technological advantages over existing systems. The incorporation of multifunctional insulating materials with other spacecraft systems can drastically reduce mass and simplify spaceship design. MLI has demonstrated the potential to provide robust MMOD protection while enabling cryogenic propellant systems(Debnath et al., 2022; Miao et al., 2022).

1.3 Aim and Objectives

This research will focus on the development of new coating materials with improved thermal insulation properties. By evaluating current insulation techniques on various materials. It will involve testing the thermal performance of different materials, such as glass bubbles, carbon fibres, glass epoxy laminates, and aerogels. This testing will be conducted under extreme temperature cycles to determine the ability of each material to maintain its insulating qualities over time.

The research objectives will involve both theoretical and experimental methods. Firstly, a literature review will be used to understand the current insulation techniques and materials used. Secondly, a 3D model of the sample slab will be developed using SolidWorks, and the samples will be tested on conditions that are relevant to the actual environment in which the spacecraft will operate using Ansys software. Thirdly, experiments will be conducted in a laboratory environment to evaluate the performance of the insulation coating under different environmental conditions. The experimental results will be compared with the Ansys simulation results to validate the model predictions. Finally, a thermographic study and flame test of the samples will be carried out to further evaluate the performance of the insulation coatings.

2 Literature Review

This overview of the literature presents the various spacecraft thermal insulation types and the state-of-the-art designs for each. Due to the extensive nature of this thesis, just the foundational principles that underpin this research are offered here.

2.1 Thermal Control Systems on Spacecraft

There are two ways in which the thermal control subsystem may function, depending on whether it is made up of passive or active components(Keesee, n.d.).

- Thermal insulation from external heat fluxes (such as the Sun or the planetary infrared and albedo flux) and adequate heat removal from internal sources both prevent the equipment from overheating (such as the heat emitted by the internal electronic equipment)(Keesee, n.d.).
- Provides additional protection from cold temperatures by isolating it from cold environments, allowing for greater absorption of heat from outside sources, or releasing heat from inside.

The thermal control systems include the followings:-

- **Environment interaction:** Interaction with the environment encompasses the way in which the exterior surfaces of the spacecraft communicate with the surrounding environment. Either the surfaces need to be shielded from the outside world, or there has to be a significant increase in the amount of contact. The primary objectives of environment interaction are to either decrease or increase the amount of heat that is lost to the surrounding environment, as well as the proportion of environmental fluxes that are absorbed(Keesee, n.d.).
- **Heat collection:** Includes the process of removing heat that has been dissipated from the equipment in which it was produced in order to prevent unwelcome rises in the temperature of the spacecraft(Keesee, n.d.).
- **Heat transport:** Transferring the heat from the location where it is produced to a device that does the radiating(Keesee, n.d.).

- **Heat rejection:** It is necessary for the heat that has been gathered and carried to be discharged at an acceptable temperature into a heat sink, which is often the environment that is around the spacecraft. The temperature at which rejection occurs is determined by the total quantity of heat that is being rejected, the temperature that has to be regulated, and the temperature of the environment into which the device is radiating heat(Keesee, n.d.)
- **Heat provision and storage:** Meaning keeping a certain temperature constant, which requires both the provision of heat and the anticipation of enough heat storage capacity(Keesee, n.d.).

2.2 Current Insulation Technologies on Spacecrafts

The current insulation technologies on spacecraft are as follows:

- **Coating:** In comparison to other TCS methods, coatings are the quickest and cheapest to implement. Coatings are placed to the spacecraft's surfaces to either decrease or enhance the rate of heat transmission. Coatings may be classified by their absorption, emission, transparency, and reflectance properties. Coatings have the fundamental drawback of deteriorating rapidly in operational environments(Aglietti, 2020; Miao et al., 2021; Rawal, 2018).
- **Multilayer Insulation(MLI):** The most prevalent kind of passive temperature management used on spacecraft is known as multilayer insulation, or MLI for short. Both heat losses to the environment and excessive heating from the environment are avoided because to MLI's insulation properties. In order to keep components of the spacecraft at the optimal temperature for operation, such as propellant tanks, propellant lines, batteries, and solid rocket motors, MLI blankets are wrapped over such components. MLI consists of three layers: the outside cover layer, the inside layer, and the interior cover layer. It is necessary for the outer cover layer to be impervious to the sun's rays, produce a negligible quantity of particle contaminants, and have the capacity to withstand the

climate and temperature to which the spacecraft will be subjected. Materials such as fibreglass woven fabric impregnated with PTFE Teflon, PVF reinforced with Nomex and bonded with polyester glue, and FEP Teflon are examples of some of the most popular materials used for the outer layer. The inner layer is required to have a low emittance as a general rule since this is one of the requirements for this layer. Mylar that has been aluminized on either one or both sides is the material that is used most often for this layer. In order to reduce weight, the internal layers are often much thinner than the outside layer. Additionally, these layers are typically perforated in order to assist in venting any trapped air during the launch process. The spacecraft's hardware is protected by the inner cover, which also serves to shield the spacecraft's more delicate internal layers. In order to avoid the possibility of electrical shorts, inside coverings are often not aluminized. Dacron and Nomex netting are two of the materials that may be found in the inside coverings. Because of safety issues, mylar is never used in production. The MLI blankets are an essential component of the system for controlling the temperature(Aglietti, 2020; Miao et al., 2021; Rawal, 2018).

- **Louver:** To regulate temperature, louvers may be employed in a variety of active ways. In addition to their usual location over exterior radiators, louvers may be installed over any apertures in the walls or floors of a spaceship to regulate the flow of air. For the same amount of energy used to keep it closed, a fully open louver is able to reject six times as much heat as a completely closed one. The bimetallic, spring-actuated, rectangular blade louver, often known as a venetian-blind louver, is by far the most popular kind of louver. The five primary components of a louver radiator assembly are the baseplate, the blades, the actuators, the sensing elements, and the structural elements(Aglietti, 2020; Miao et al., 2021; Rawal, 2018).
- **Heaters:** An important part of thermal control design is the use of heaters to mitigate the effects of cold-case environments on components and to compensate for insufficient heat transfer. To precisely regulate the

temperature of a specific component, heaters are paired with thermostats or solid-state controllers. Heaters are also often used to bring cold components up to their bare minimum operational temperatures before they are switched on. Patch heaters, which consist of an electrical-resistance element sandwiched between two sheets of flexible electrically insulating material like Kapton, are by far the most prevalent form of heater used aboard spacecraft. Depending on the need for fault tolerance, the patch heater might have either a single circuit or many circuits (Aglietti, 2020; Miao et al., 2021; Rawal, 2018).

Cartridge heaters are another common form of heating device, often used to preheat high-temperature components like propellants or large blocks of material. For this heater, a coiled resistor is housed in a cylindrical metal housing. To use a cartridge, a hole is typically bored into the component being heated, and the cartridge is then potted into the hole. Heaters in cartridge form typically have a diameter of a quarter inch or less and a length of a few inches at most. Radioisotope heater units, or RHUs for short, are another form of spaceship heater. Due to the very low sun brightness, which significantly lowers the electricity provided by solar panels, RHUs is utilised to reach worlds beyond Jupiter. These heaters may be used anywhere on the spaceship since they operate independently of the ship's electrical system. Each RHU gets its heat from the decay of a radioactive substance. Plutonium dioxide is the main ingredient. One RHU is quite portable, weighing in at just 42 grammes and fitting inside a cylindrical case about 26 mm in diameter and 32 mm in length. At the moment of encapsulation, each unit produces 1 W of heat, although this heat output gradually diminishes with time. The Cassini mission used 117 RHUs(Aglietti, 2020; Miao et al., 2021; Rawal, 2018).

- **Radiators:** Radiators release into space the spacecraft's excess waste heat. There are a few distinct types of radiators, including panels built into the spacecraft itself, flat-plate radiators attached to the outside of the vehicle, and panels that are deployed after the craft has reached orbit. It doesn't matter how they're set up, radiators all function by reflecting

infrared (IR) light away from their surfaces. The emittance and temperature of a surface determine its radiative power. The radiator has to get rid of the heat coming off of the spaceship and any heat coming in from the outside in the form of radiation. Therefore, most radiators have surface finishes with low solar absorption to minimise heat from the Sun and high IR emittance to maximise heat rejection. Typically, spacecraft radiators dump between 100 and 350 W per square metre of heat produced by the spaceship's electronics. An existing structural panel may be utilised as a radiator with essentially no additional weight, whereas a hefty deployable radiator and its support structure can add up to roughly 12 kg/m2.

In this view, the radiators of the International Space Station stand out as a series of white square panels bolted to the main truss (Aglietti, 2020; Miao et al., 2021; Rawal, 2018).

- **Heat Pipes:** Heat pipes are a kind of passive thermal energy transmission that move huge amounts of heat between two points using a closed two-phase liquid-flow cycle comprised of an evaporator and a condenser. Constant conductance heat pipes (CCHPs) and axial groove heat pipes (AGHPs) are aluminium extrusions that employ ammonia as the working fluid, and they are designed for use in aerospace applications. Common uses for this technology include improving the efficiency of radiator panels and managing the temperature of a ship's payload(Aglietti, 2020; Miao et al., 2021; Rawal, 2018).

2.3 Materials and Properties

This section navigates through the different materials used in the research and their properties.

- **Carbon Fibres:** Carbon fibres or carbon fibres (alternatively CF, graphite fibre or graphite fibre) are fibres comprised primarily of carbon atoms and measuring between 5 and 10 micrometres (0.00020–0.00039 in) in diameter. Carbon fibres have numerous benefits, including high rigidity, high tensile strength, a high strength-to-weight ratio, good chemical

resistance, high-temperature tolerance, and minimal thermal expansion. Carbon fibre is widely used in aerospace, civil engineering, the military, motorsports, and other competitive sports because to these qualities. Nonetheless, they are more expensive than comparable fibres such as glass fibre, basalt fibre, and plastic fibre(Goodhew et al., 1975; Yum et al., 2015).

Typically, carbon fibres are mixed with other materials to create composites. When carbon fibre is impregnated with a plastic resin and baked, it forms carbon-fibre-reinforced polymer, which has a very high strength-to-weight ratio and is exceedingly rigid despite being slightly brittle. Carbon fibres are frequently combined with other substances, such as graphite, to create carbon-carbon composites with a very high heat resistance (Goodhew et al., 1975; Yum et al., 2015). The properties are shown in Table 2

Table 2 Properties of Carbon Composite(Goodhew et al., 1975)

Property	Carbon Composite
Compressive strength	615MPa
Tensile strength	645MPa
Tensile modulus	55.2GPa
Flexural strength	882MPa
Strain to failure	1.5%
Tg – Storage Modulus Onset	140 C
Tg – Tan δ Peak	148 C
Flexural modulus	60.1GPa
Interlaminar shear strength	69.8MPa

- **Glass Epoxy Laminate:** Advanced Materials utilises a wide variety of technological composites based on glass fibre and high-performance epoxy resin. Products in this category may be used in a broad range of high-temperature contexts. Insulation against heat and electricity is maintained to a perfect degree in glass-epoxy composites. They may be used in situations where high-temperature resistance, dimensional stability, and mechanical strength are required since their flammability is within the user's control. A glass-fibre matrix and epoxy resin form the composite material that makes up this product. In order to create epoxy or polyoxide, epoxide monomers are polymerized with a hardener to form a resin. Heat is used to induce a curing effect(Gordon et al., 2023; Rawal, 2018; Yum et al., 2015). E-6000 glass epoxy plates are one of two available varieties and include low heat conductivity (0.25 W.m-1. K-1) and low density to make it possible to create thinner, lighter insulating components. It can withstand 220 degrees Celsius in constant heat and 320 degrees in a short burst of time. Glass-fibre matting and a light-yellow epoxy resin serve as the base for this laminate. In tests, it proved to be very resistant to chemicals (Gordon et al., 2023; Rawal, 2018; Yum et al., 2015). The properties are shown in Table 3

Table 3 Properties of Epoxy Laminate (Gordon et al., 2023)

Property	Glass Epoxy Laminate
Fibre Volume ratio	65%
Density	1800Kg/cm^3
Longitudinal modulus	40.51GPa
Transverse modulus	13.96GPa
Transverse tensile strength	64MPa

Longitudinal tensile strength	783MPa
Poisson's ratio	0.22
Shear strength	69MPa
Interlaminar shear strength	38MPa

- **Glass Bubbles:** Glass bubbles, often known as glass microspheres or micro balloons, are used to bulk out or thicken resin systems such as epoxy, polyurethane, and polyester. This lowers their density and makes them simpler than sand. Other names for glass bubbles include glass microspheres and micro balloons. When added to laminates, they have the potential to offer a smoother surface, and when used in castings, they have the capacity to increase dimension stability while simultaneously decreasing the weight and cost of the completed product(Cornaro & Buratti, 2020; Shahedan et al., 2021).

  When you mix microspheres with epoxy, you get a filler that is both very light and very strong. When mixed with polyester or epoxy, they make a coating that is easy to sand after it has been applied. Genuine 3M K series glass bubbles have a relative density of 0.2 grammes per cubic centimetre and conform to the K20 standard for glass bubbles. Up to a maximum proportion of around 15-20% by weight, glass bubble filler may be applied to most resin systems (including epoxy, polyester, and polyurethane). Because they are round and made of different chemicals, glass bubbles can withstand high pressures that come from the outside. The strength of glass bubbles is measured in terms of their isostatic crush strength, which ranges from 100 to 30,000 pounds per square inch (PSI) depending on the grade. Because the crush strength of a certain grade is highly dependent on the wall thickness, there is an inverse relationship between the density

of the grade and the crush strength of the grade (Cornaro & Buratti, 2020; Shahedan et al., 2021).

Glass bubbles have become important fillers in the composites industry because of their small size, high strength, and very low density. This has allowed them to stand out from other types of fillers. As we have shown, the insertion of glass bubbles into composite components may bring a range of benefits in addition to those associated with light weighting, including advantages in terms of processing as well as functioning. This is a commonly accepted fact. In actual production, composite manufacturers often take advantage of many of these advantages of glass bubbles at the same time (Cornaro & Buratti, 2020; Shahedan et al., 2021). The properties are shown in Table 4

Table 4 Properties of Glass Bubbles(Shahedan et al., 2021)

Property	Glass Bubble
Shape	Hollow spheres with thin walls
Composition	Soda-lime-borosilicate glass
Colour, unaided eye	Off-white, powdery
Crush strength (90% survival)	250–27,000 psi / 17–1860 bar
True density	0.125–0.60 g/cm3
Median particle size	18–65 microns
Softening temperature	600ºC (1112ºF)
Thermal conductivity	0.05–0.20 W/m.K @ 20°C
Dielectric constant (@ 100 MHz)	1.2–1.9

- **Aerogel**: Aerogel is a unique material that is commonly referred to as "frozen smoke" or "solid air." Both of these descriptions are accurate. In a manner analogous to that of a sponge, it is composed of a network of interconnected nanoparticles and has the properties of being transparent, lightweight, and extremely porous. There is a wide variety of raw materials that can be used to manufacture aerogels, including silica, metal oxides, and polymers(Gurav et al., 2010; Shen et al., 2013; Universités et al., 1987).

  Because aerogels can be composed of up to 99.9 percent air, they have a very low density, which is what gives them their distinctive quality. Due to the fact that they have the lowest thermal conductivity of any solid material, they are one of the most effective insulators that can be found anywhere in the globe. They also have a high degree of transparency, which makes them an excellent choice for use as windows because they insulate against the heat while letting natural light shine through.

  Aerogels have a wide range of potential uses, from the aircraft industry to the architectural industry. For example, they are utilised in the process of insulating spacecraft, which is an essential component in the process of shielding the vehicles from the intense heat and cold of space. In addition to this, they are utilised in the insulation of buildings so that energy efficiency may be increased and CO2 emissions can be decreased. In the oil and gas business, for example, they are used to absorb oil spills and improve oil recovery rates. This is one of the industries in which they are useful (Gurav et al., 2010; Shen et al., 2013; Universités et al., 1987).

  Despite their many benefits, aerogels are still relatively expensive to produce, limiting their usage in many industries. Nevertheless, researchers continue to develop new methods for synthesizing aerogels and exploring their potential applications.

Aerogels are a type of material that, on their own, have a property of being hydrophilic. This means that they have a natural affinity to absorb moisture from their surroundings. However, this property can be problematic, as when they do absorb moisture, they undergo a structural change that can cause contraction and overall deterioration. This can be particularly troublesome in certain applications, such as insulation, where maintaining the structural integrity of the material is crucial.

One way to address this problem is by rendering the aerogels hydrophobic, or water-repellent, through the use of a chemical treatment. This treatment alters the surface of the material in such a way that it no longer has a tendency to absorb moisture. In turn, this helps prevent the aerogels from undergoing structural changes and deteriorating.

Importantly, not all hydrophobic treatments are created equal. In some cases, simply adding a hydrophobic layer to the outside of the material is not enough to protect the aerogel from degradation. Instead, it is more effective to treat the entire core of the material with a hydrophobic coating. This creates a layer of protection that extends throughout the entire structure, reducing the likelihood of degradation in the event that a crack develops on the surface of the material (Gurav et al., 2010; Shen et al., 2013; Universités et al., 1987).

Overall, while aerogels have many desirable properties, their hydrophilic nature can make them susceptible to degradation over time. By applying a hydrophobic coating, however, their structural integrity can be maintained, making this unique material suitable for a wide range of applications.The properties are shown in Table 5

Table 5 Properties of Aerogel(Gurav et al., 2010)

Property	Aerogel
Thermal conductivity at P_{atm}	18 to 20 mW/m.K-1 (20°C)
Service temperature at P_{atm}	-160 to 400°C
Particle size	Up to 3500 µm
Apparent density	60 to 90 kg/m^3
Tapped density	1,1 x Apparent density
Surface chemistry	Hydrophobic - Corrosion resistant
Pores diameter	5 to 12 nm
Mercury porosity	90 to 98%
Specific surface (N2 BET)	750 to 950 m2 /g
pH stability range	1 to 9 included
Minimum ignition temperature	470°C
Heat capacity at 20°C (Cp)	1582 J/kg.K^{-1}
Resistivity	5.9x10^{13} Ω.m
Emissivity	0.93
Particle compressive strength	0.3 to 0.8 MPa

2.4 State of Art Coating Techniques

Spacecraft use a range of thermal insulation materials with different properties and applications to protect against the extreme temperature variations that occur during a mission. These materials include polyimide foam, silica aerogels, and multi-layer insulation.

Polyimide foam is lightweight and flexible, with excellent thermal and mechanical performance, making it ideal insulation for space probes and satellites. Silica aerogels are another high-performing insulation material that provides excellent thermal resistance, transparency, and durability. These properties make it ideal for use in transparent windows of space shuttles and spacecraft(Babels et al., 1996; Johnson et al., 2003).

Multi-layer insulation (MLI) is another commonly used thermal insulation coating method in spacecraft. It consists of multiple layers of reflective film, which prevents radiative heat transfer by bouncing the heat back into space, making it ideal for protecting sensitive electronic equipment and spacecraft from the harsh environment of space(Babels et al., 1996).

In conclusion, the state of the art in coating for high-performance thermal insulation in spacecraft depends on the mission's requirement and thermal environment. The insulation material and coating method must work together efficiently to ensure the spacecraft's safe operation in extreme temperature conditions.

2.5 Various Methods of Thermal Evaluations

This section will navigate through the different thermal evaluation methods, which are as follows:

- **Thermal conductivity measurement:** Measuring thermal conductivity entails measuring the rate at which heat travels through an insulating medium. A thermal conductivity metre is employed to determine the rate of heat transmission through the insulation. The better the insulating characteristics of a substance, the lower its heat conductivity(Y. Zhang et al., 2017).
- **Thermogram analysis:** A high-resolution infrared camera can be utilised to measure the temperature of the insulation material. The distribution of temperature over the insulation can be utilised to evaluate its thermal performance. The use of thermograms permits the identification of hotspots on the surface of the insulation (Y. Zhang et al., 2017).

- **Differential scanning calorimetry (DSC):** This technique measures the thermal properties of the insulating material, including its heat capacity, thermal conductivity, transition temperatures, and enthalpy changes. In a controlled setting, the material is heated and cooled, and the heat flow during each stage is measured. The DSC offers information regarding the material's response to changes in temperature (Y. Zhang et al., 2017).
- **Thermal stress testing:** The thermal stress test examines the thermal stability of the insulation material under harsh environmental conditions. To imitate the circumstances of a space flight, temperature cycling and thermal shocks are applied to the insulation. The approach identifies any material degradation, delamination, or cracking that may occur as a result of variations in temperature (Y. Zhang et al., 2017).
- **Thermal vacuum testing:** This procedure involves exposing the insulation material to varying temperatures in a vacuum atmosphere. The thermal conductivity, deterioration, and mechanical properties of the insulation are then examined. The vacuum environment simulates the circumstances of the space environment, where high levels of vacuum and fluctuations in temperature might impair the insulation's performance (Y. Zhang et al., 2017).
- **Burn Test:** The burn test measures the flammability of a material by exposing it to a high temperature and igniting it. It is an effective way to determine the behaviour of materials under fire conditions and how they react to heat. The thermal response of a material during a burn test provides data on the heat transfer rate, the flame spread, the amount of smoke produced, and the time it takes for the material to ignite and burn (Y. Zhang et al., 2017).

2.6 Research Gap

Currently, spacecraft are intended to resist the extreme temperature, pressure, and radiation found in space. Thus, a crucial aspect of spacecraft design is its

heat management system, which ensures the safe operation of sensitive equipment, electronics, and humans on board.

Hence, thermal insulation is essential for maintaining the ideal temperature within a spaceship by limiting unwanted heat transmission between the inside and exterior of the vessel. Standard spacecraft insulation materials include aerogels, silica felts, and multi-layered blankets.

To attain greater thermal insulation performance for sustainable space exploration, however, it is necessary to overcome the constraints of current insulation materials. For example, aerogels are fragile and expensive to manufacture. Silica felts are hefty and incapable of withstanding intense radiation. Multiple-layered blankets are cumbersome and susceptible to compression, which reduces their thermal insulation effectiveness.

Consequently, the research gap in high-performance thermal insulation in spacecraft is the development of innovative materials that combine lightweight, durability, and high thermal insulation properties, are easy to install and maintain, and are resistant to harsh space environment conditions such as radiation, vacuum, and extreme temperatures.

The development of high-performance insulating materials will allow future spacecraft to function more efficiently, minimise the need for bulky thermal shielding, increase mission duration, and enhance crew safety and comfort.

3 Methodology

This section describes the different stages of this research as follows:

- Evaluating current insulation on spacecraft
- Accessing different materials used for coating
- Current insulation problems
- Design specification
- Design variable selection
- Developing a 3D slab model
- Ansys modelling and testing
- Solver Results
- Material selection
- Desired Thickness of material
- Experimentation of coating on a composite with environmental conditions
- Mechanical testing of the composite with coating
- Final evaluation for prototype

The initial step was doing an analysis of the many sustainable designs that are now in use, after which the data was collected and recorded. During the second stage, an analysis of the spacecraft's existing insulation was performed, and the details were taken down. The third stage consisted of doing an analysis of the existing issues that the spacecraft was contending with and making notes for the sake of future material selection and design specification. The design specification for the analysis was finalised at the fourth stage of development. The selection of the design variables took place at the fifth step of the process. In the sixth step, a three-dimensional slab model was created for the purpose of analysis. This model included all of the design variables and requirements up to that point. ANSYS software was used as solver on this model, taking into account all of the environmental factors in the seventh step. The eighth and final step is the outcome; this stage included parametric procedure that continued until a suitable material selection and thickness were discovered. The last step consisted of an assessment of the findings utilising all of these factors, after which

it was proposed that future research should focus on creating more complicated structures

3.1 Theoretical Calculation

This section describes the experimental calculation carried out to achieve the modelling data for this research. A schematic representation model as shown in Figure 2

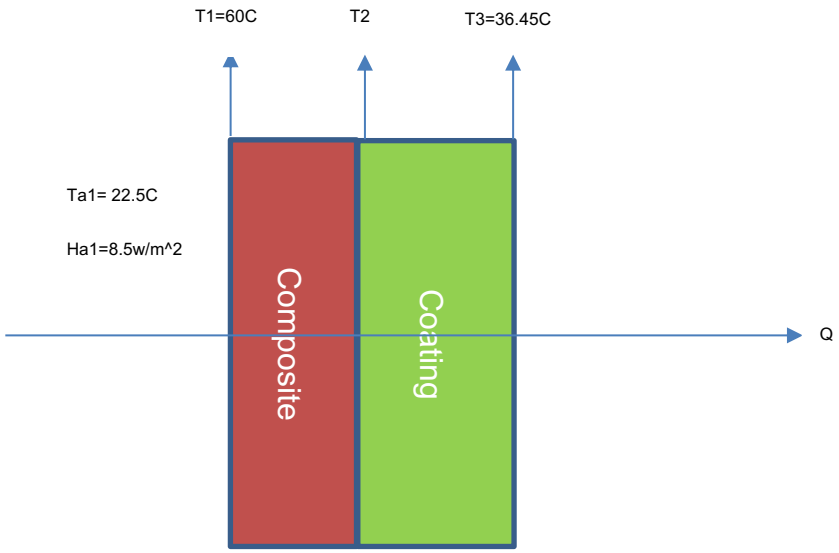

Figure 2 Schematic Representation of Model

Considering the model is 1-D calculation and steady-state thermal analysis

Thermal conductivity of Glass Plate K_P = 0.22 W/mK

Total area **A**= 0.01m^2

The thickness of composite L_P= 0.002m

The thickness of coating L_C= 0.005m

Temperature of coating T_3 = 36.45C(from experiment)

Perimeter **P**= 0.4 m

Surface heat transfer coefficient

$$\mathbf{H} = \mathbf{1.32} * \left(\frac{\Delta \boldsymbol{T}}{\boldsymbol{D}}\right)^{\mathbf{0.25}} \qquad \textbf{Equation 1}$$

$$\mathbf{D} = \frac{\boldsymbol{4A}}{\boldsymbol{P}} = \mathbf{0.1} \qquad \textbf{Equation 2}$$

Since the plate is getting heated from the bottom side Equation 1can be used to find the heat transfer coefficient (Nicolai' & De Baerdemaeker, 1996).

Surface heat transfer coefficient H= 4.53 W/mK

Using newton's law of cooling we get overall heat transfer as shown Equation 3

$$\boldsymbol{Q} = \boldsymbol{H} * \boldsymbol{A} * (\boldsymbol{T_3} - \boldsymbol{T_1}) = \mathbf{0.63W} \qquad \textbf{Equation 3}$$

Heat Transfer

$$= \frac{(\boldsymbol{T_1} - \boldsymbol{T_2})}{\boldsymbol{R}} \qquad \textbf{Equation 4}$$

$$= \frac{\boldsymbol{t_p}}{\boldsymbol{K_P} * \boldsymbol{A}} = \mathbf{0.90\ W/K} \qquad \textbf{Equation 5}$$

From Equation 3 and Equation 4 we get;

$$\boldsymbol{T_2} = \mathbf{59.43}\boldsymbol{C}$$

Thermal conductivity of coating

$$= \frac{\boldsymbol{Q} * \boldsymbol{L_C}}{\boldsymbol{A} * (\boldsymbol{T_2} - \boldsymbol{T_3})} = \mathbf{0.0137\ W/mK} \qquad \textbf{Equation 6}$$

Equation 6 was used to determine the thermal conductivity of the samples; this equation describes the steady-state, one-dimensional heat conduction through a plane wall and is written in the form wherein k is the thermal conductivity of the sample, Q is the rate of heat flow (conduction) across the sample, A is the cross-sectional area, T is the temperature difference across the sample, and L is the thickness(Nicolai' & De Baerdemaeker, 1996).

A material with a known thermal conductivity value was employed (as a reference) and the temperature at the top and bottom of the sample was recorded in order to compute the amount of heat movement across the sample, which is denoted by the letter Q. Due to the fact that the thermal conductivity was already known, Q could be determined for a variety of temperatures by applying. Following the aforesaid procedure, three separate runs were carried out at the temperature that was specified, and the average Q value for each temperature was utilised for the subsequent calculations regarding the samples' thermal conductivity(Nicolai' & De Baerdemaeker, 1996).

3.2 Modelling and Analysis

This section describes the modelling and analysis carried out to achieve the modelling data for this research.

3.2.1 3D Modelling

SOLIDWORKS was used for the modelling process. The specs and measurements were used to create a detailed 3D model of the body chamber. Due to the complexity of the body chamber model, a 3D slab model was created and all design variables were transferred across. The slab was manufactured to

two distinct standards and then joined together. Here's what we did with our design variable: -

- Length 100mm
- Width 100mm
- Thickness 1 – 2mm
- Thickness 2 – 5mm

The primary composite material (thickness 1) and the thermal insulation layer (thickness 2) are both described here. Both the composite material slab model and the thermal insulation slab model may be seen in.

The steps used to create a 3D slab model are as follows

- Open SolidWorks and create a new part file
- Select the "Sketch" icon and create a sketch on the "Front" plane
- Draw a rectangle using the "Rectangle" tool, specifying the dimensions of the slab
- Use the "Extrude" tool to extrude the rectangle to the desired thickness
- Save the final model as a part file for future use
- Repeat steps again from 1 to create another slab.
- Now, open Solid Works again and Use the Insert Component option to insert the second slab into the assembly
- Use the Move Component option to align the two slabs as needed
- Use the Mate option in the Assembly tab to fix the two slabs in place. You can choose from various mate options such as coincident, parallel or perpendicular
- Once the two slabs are mated, save the assembly file

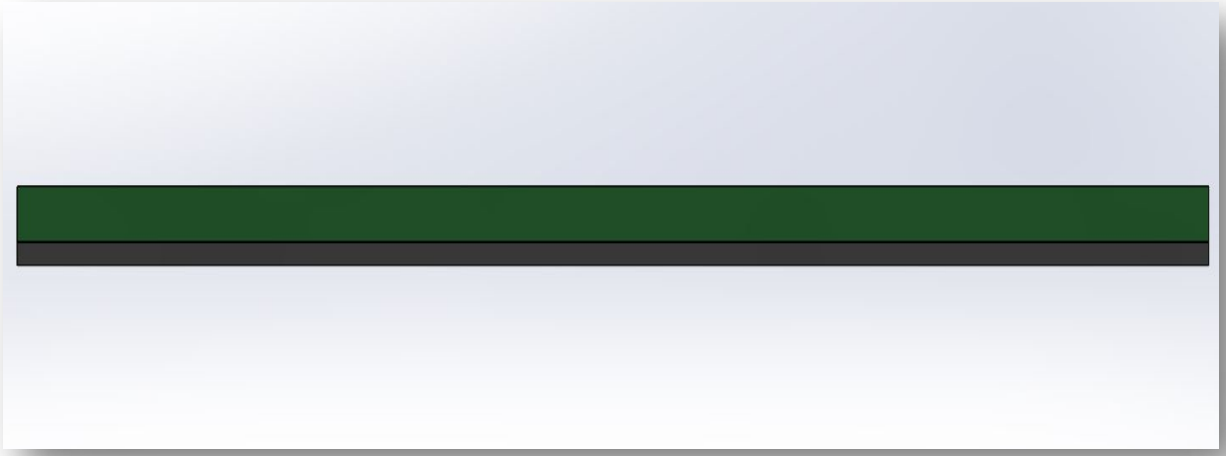

Figure 3 3D Slab Model Using Solid Works

The above Figure 3 shows the 3D model of the sample for the experimental work. The dimension of the composite slab is 100 X 100 X 2 mm which is shown in grey in colour and the coating is 100 x 100 x 5mm which is shown in green in colour.

3.2.2 Thermal and Mechanical Analysis

Mechanical and thermal analyses were performed with the help of ANSYS Workbench. We have chosen our materials and put their attributes into the programme. Composite-Aerogels were employed as the combined material type. The solid works file was loaded into ANSYS to create the 3D slab. Transient thermal analysis was used on the 3D model under all imaginable situations to provide temperature profiles for each possible permutation. Static structural analysis was used to conduct the mechanical study, and identical characteristics and conditions were used in both analyses. The results include all the information that was gathered. To perform steady-state thermal analysis in ANSYS Workbench with a thermal load for 1200 seconds Table 6, follow these steps:

- Create a new project in ANSYS Workbench
- Import the geometry and mesh it Figure 4
- Add a thermal load to the model
- Specify the material properties
- Set up the analysis type as steady state thermal Figure 5

- Define the boundary conditions
- Mesh the model
- Run the simulation for 1200 seconds

To apply a heat flux, go to the boundary condition tab and select the surface where the heat flux needs to be applied. Specify the value of the heat flux from theoretical calculation, and its direction. The parameters are shown in below

Table 6 Parameter for Solver

Analysis Type	Steady state thermal analysis
Co-ordinate System	12 Nodes
Mesh Type	Edge Sizing
Initial Temperature	15^{o}C
Boundary Condition	Temperature load and Convection on top face
Step Time	1200 seconds
Solvers	Temperature, Maximum Shear Stress and Total Deformation

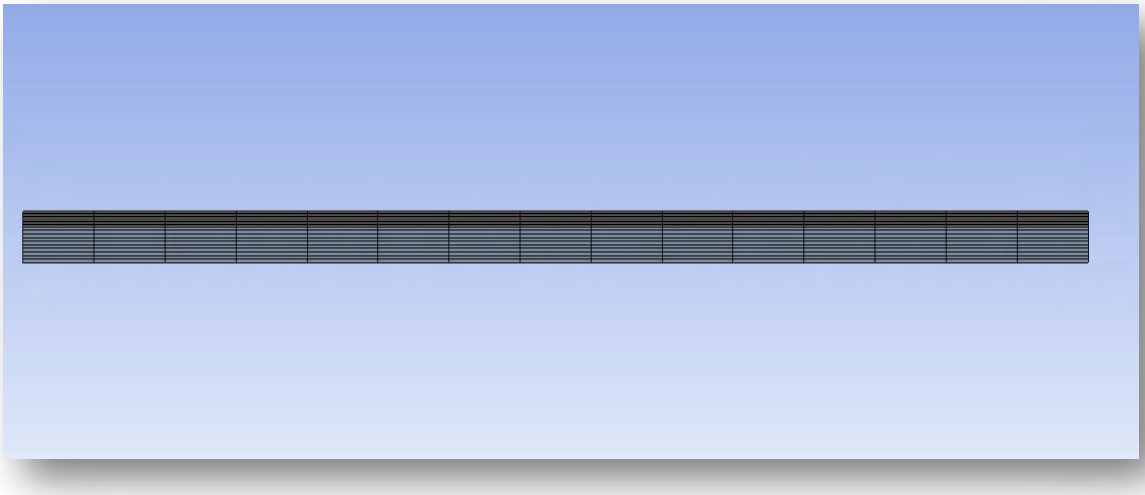

Figure 4 Image of Meshing in ANSYS

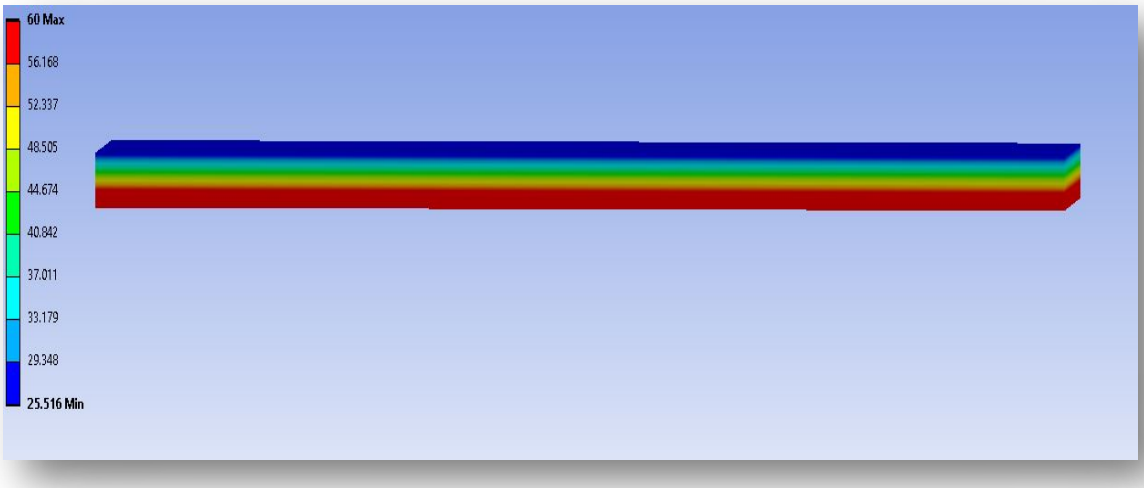

Figure 5 Image of Temperature Analysis

3.3 Solver Results

This section navigates through comparative results obtained from the ANSYS software.

3.3.1 Modelling Results

This section explains the modelling results from ANSYS Software.

The ANSYS programme used to get the information that is now being shown here as the results. The findings shown here are those obtained by combining Composite and Aerogel. The thickness of the aerogel coating is 5 millimetres, while the anticipated thickness of the composite is 2 millimetres. After analysing the data with the different environmental conditions, these final thicknesses were obtained.

The Figure 6 material attributes were entered into the programme, and the results may be broken down as follows.is the temperature difference between the composite and the aerogel coating if the coating is 5 millimetres thick.

The coating has a thickness of 5 millimetres, which is more than sufficient to bring the surface temperature of the coating down to 30 degrees Celsius. This temperature is the maximum temperature that the composite and the other components on the interior can endure. In order to ensure that it is clear that the aerogel needs just a thin layer of coating to be applied.

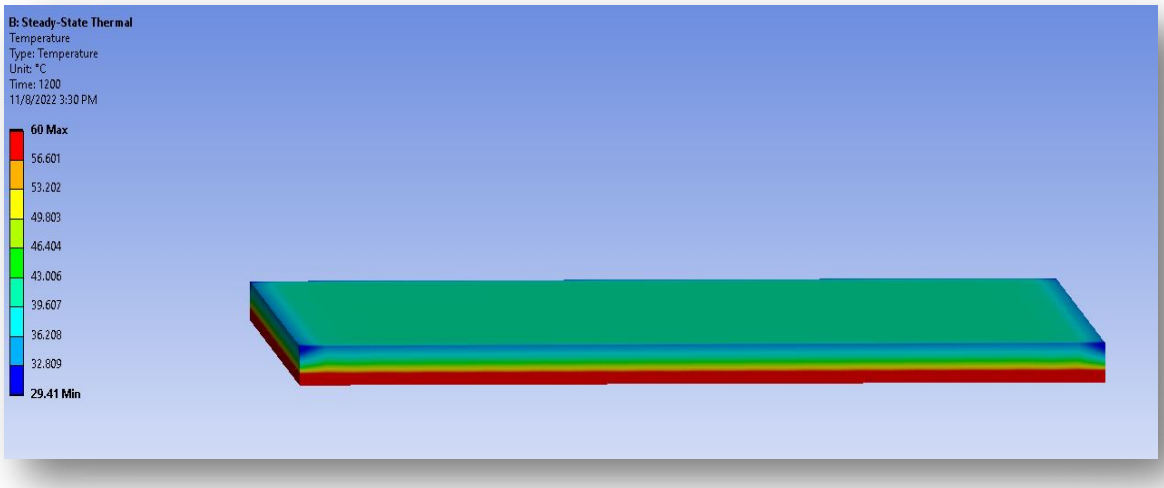

Figure 6 Steady state Thermal Analysis

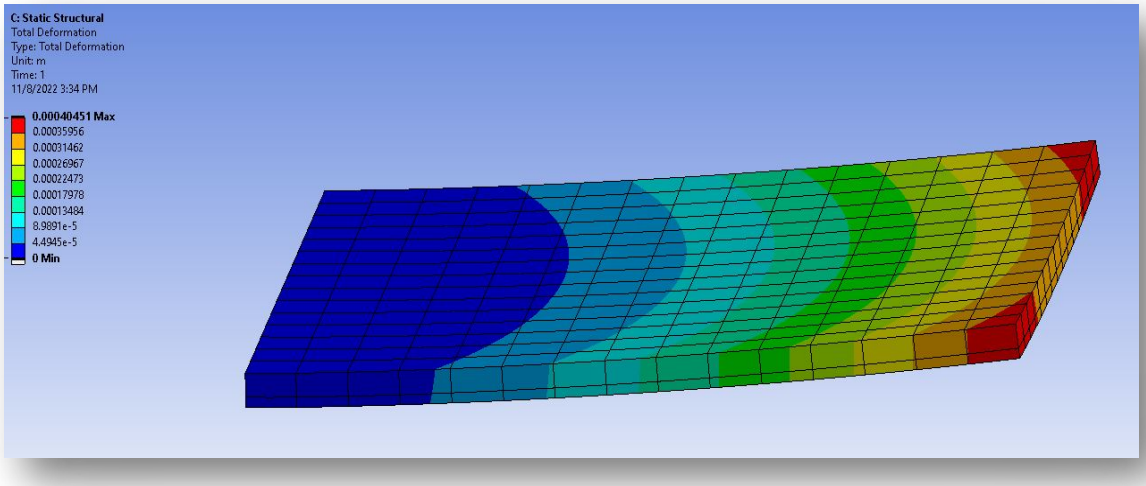

Figure 7 Total Deformation of Aerogel Coating

Figure 7 depicts the overall deformation of the composite after it was coated with aerogel. With all of these environmental circumstances, the greatest amount of deformation that may occur as a result of this combination is 0.0079 mm of expansion. Under conditions of purely thermal stress, all of these results were

discovered. It has a lower rate of thermal expansion when compared to the expansion rate of other coatings.

3.3.2 Comparative Image from Solver Results

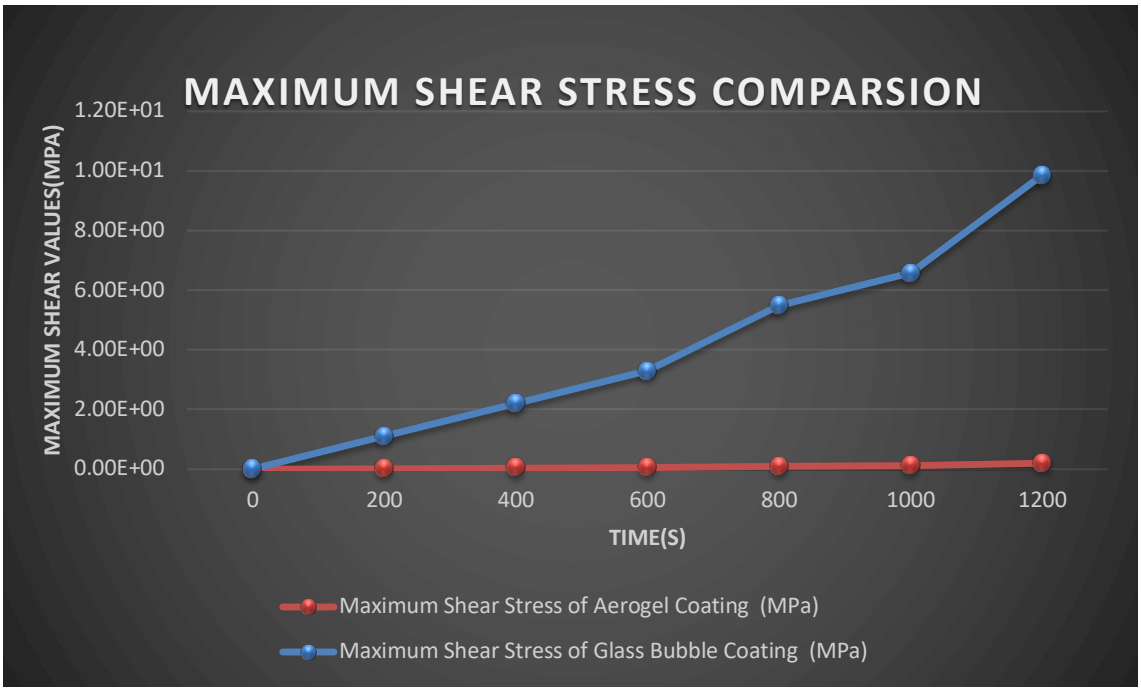

Figure 8 Comparison of Maximum Shear Stress

Figure 8 is a graph illustrating a comparison of the maximum shear stress shown by the composite whether coated with glass bubbles or aerogel. When compared to the composite that was coated with aerogel, the graph shows that the composite t was coated with glass bubbles sheared more. In a composite with a glass bubble coating, the highest shear stress is 9.86 MPa, but in a composite with an aerogel coating, the maximum shear stress is just 0.203 MPa. When compared with composites that have glass bubble coating, shear rates are lower for materials that have an aerogel coating.

According to the data obtained as a whole, aerogel coating with composite is superior to composite with glass bubble coating in each and every scenario.

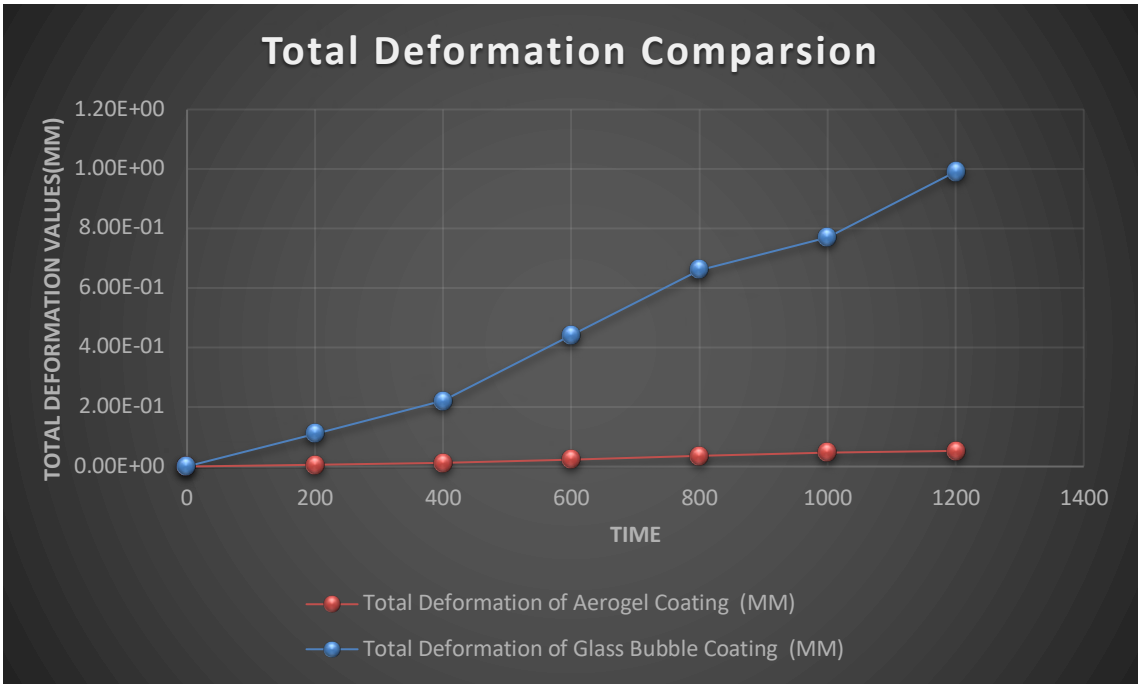

Figure 9 Comparison of Total Deformation

Figure 9 is a graph illustrating the comparison of the composite with the glass bubble coating and the aerogel coating. In accordance with the data shown in the graph, the composite with the glass bubble coating deforms more than the composite with the aerogel coating. In the case of a composite with an aerogel coating, the maximum distortion is just 0.0527 millimetres, but the greatest deformation for a composite with a glass bubble coating is 1 millimetre. When compared with composites with glass bubble coating, the rate of deformation is lower for composites with aerogel coating.

3.4 Laboratory Experimental Methods

This section describes the experimental works carried out using modelling data for this research.

3.4.1 Experimental setup

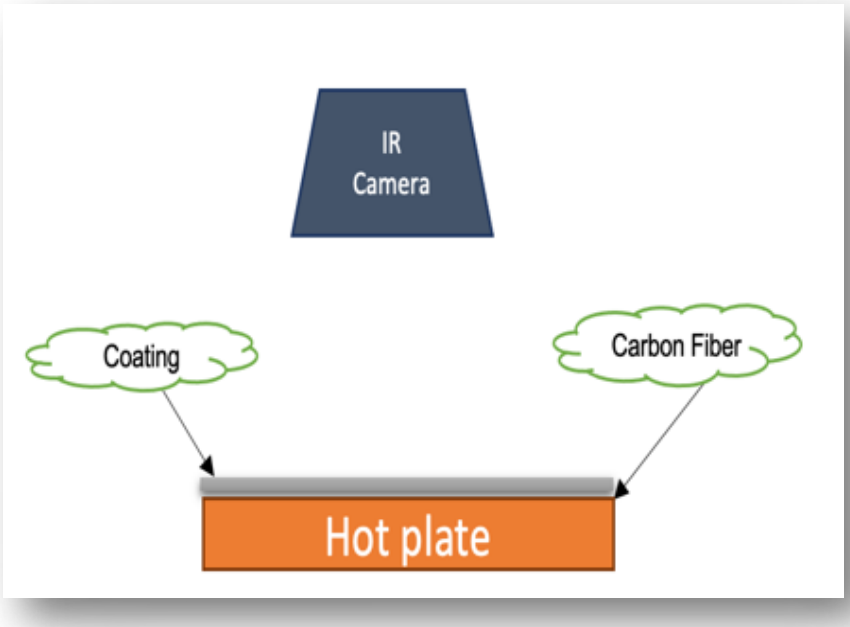

Figure 10 Schematic Prestation of the Setup

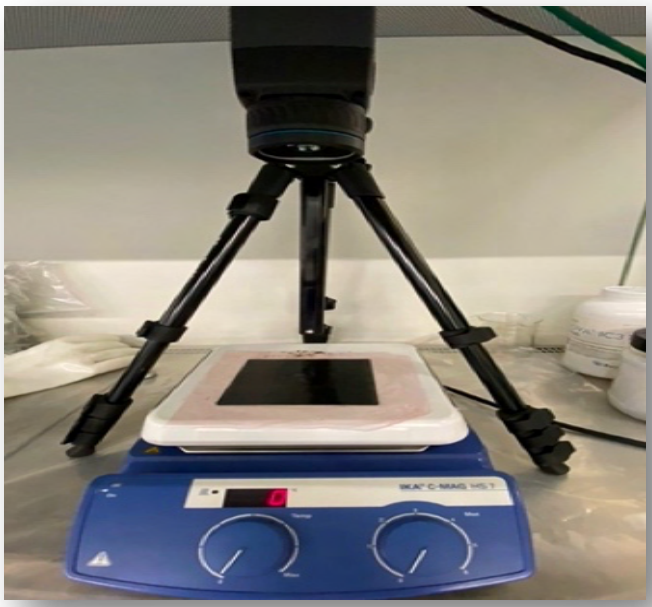

Figure 11 Actual Setup

The Experiment is conducted in a fume cabinet. The sample is kept directly on the hot plate and heated till 60^{o}C . The thermal images are captured at different time intervals. The thermal camera used here is FLIR A655 with 95% emissivity. A schematic representation of the setup is shown in Figure 10 and the actual setup is shown in Figure 11. Thermal imaging, also known as thermography, is a technique that allows you to capture images of objects based on their temperature differences. A thermal camera is a device that can detect and measure infrared radiation, which is emitted by objects based on their temperature.

To capture thermal images of samples using a thermal camera, follow these steps:

- Set up the thermal camera: Ensure that the camera is calibrated and ready to capture images. The camera should be set to the appropriate temperature range for your samples.
- Prepare the samples: The samples should be at a stable temperature and should not be moved or disturbed during the imaging process.
- Capture the thermal images: Point the thermal camera at the samples and capture the images. Ensure that the camera is focused on the samples and that the images are clear and in focus.
- Analyse the images: Use image analysis software to analyse the thermal images and extract temperature data from the samples. You can also use the software to create visual representations of the temperature data, such as thermal maps or temperature profiles.

Thermal imaging can be used in a variety of applications, including material testing, product development, and medical imaging. It can provide valuable insights into the temperature distribution of objects, which can be used to optimize processes, identify defects, and improve product performance. The thermal camera specification is shown in below Table 7

Table 7 Thermal Camera Specifications

Resolution	640 × 480
Detector Pitch	17 μm
Spectral Range	7.5 – 14.0 μm
Detector Type	Uncooled Microbolometer
Camera f-number	f/1.0
Dynamic Range	16-bit
NETD	<30 mK
Frame Rate [Full Window]	50 Hz
Max Frame Rate [at Min Window]	200 Hz (640 × 120)
Standard Temperature Range	40°C to 150°C (–40°F to 302°F) 100°C to 650°C (212°F to 1,202°F)
Optional Temperature Range	Up to 2,000°C (3,632°F)
Focus	Automatic or Manual (Motorized)

3.4.2 Design of Experiment

SolidWorks was used to build a frame that could hold the sample while the coating was applied to get the best possible surface and edge finishing. As in the, the frame was produced by a 3D printer.

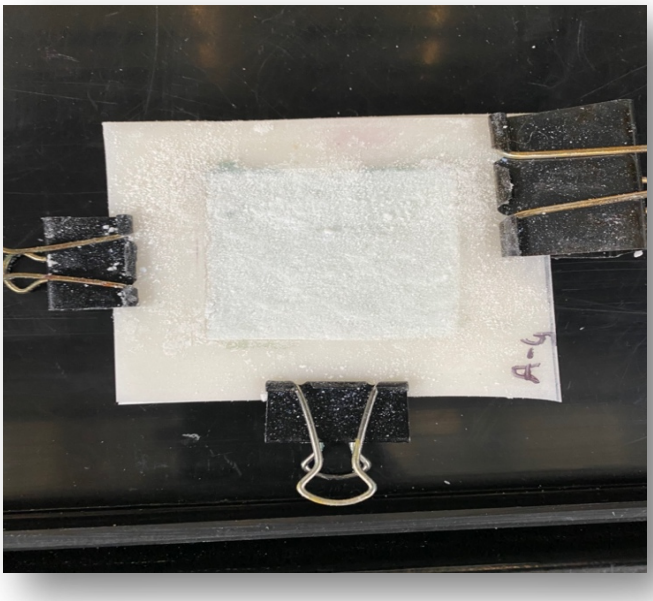

Figure 13 Frame with Sample

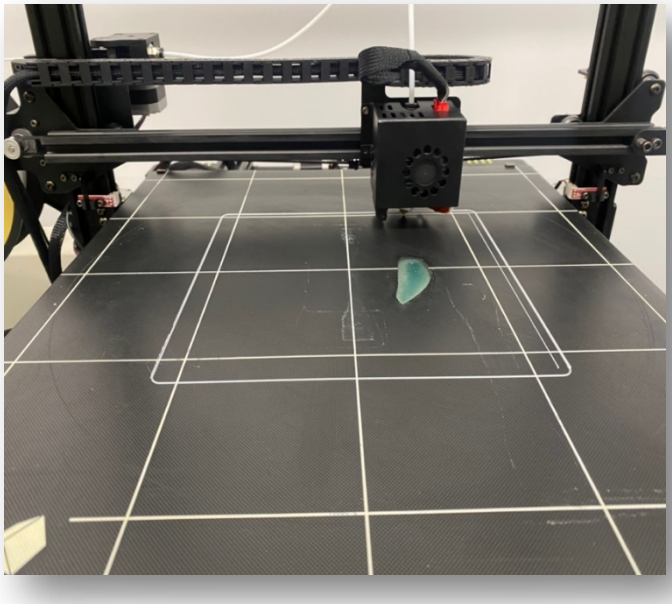

Figure 12 3D Printing of Frame

The Figure 12 shows the printing process of the frame used for holding the sample. And Figure 13 shows the frame holding sample for easy application of coating to the sample.

3.4.3 Experimental Preparations

Researchers came to the conclusion that mixing aerogel and binder in an equal percentage of 50:50 based on the results of a number of separate studies and an analysis of the data that was linked with those trials. In order to conduct an analysis of the effects of using various binders, the following three cases were obtained:

Case 1: -

- Aerogel blend is prepared in a ratio 50:50
- 50% by volume of aerogel powder and 50% of granules are mixed with ethanol.
- The above blend is mixed with epoxy at a proportion of 70:30
- A 5mm layer of coating is applied on top of the composite and left for curing for 24hr in room temperature.

Case 2: -

- Glass bubble blend is prepared in a ratio 50: 50

- 50% by volume of Glass bubble fine powder and 50% of Glass bubble rough particles are mixed with ethanol
- The above blend is mixed with epoxy at a proportion of 70:30
- A 5mm layer of coating is applied on top of the composite and left for curing for 24hr in room temperature

Case 3: -

- Aerogel and Glass Bubble is prepared in a ratio 50: 50
- 50% by volume of aerogel powder and 50% of glass bubble are mixed with ethanol.
- The above blend is mixed with epoxy at a proportion of 70:30
- A 5mm layer of coating is applied on top of the composite and left for curing for 24hr in room temperature.

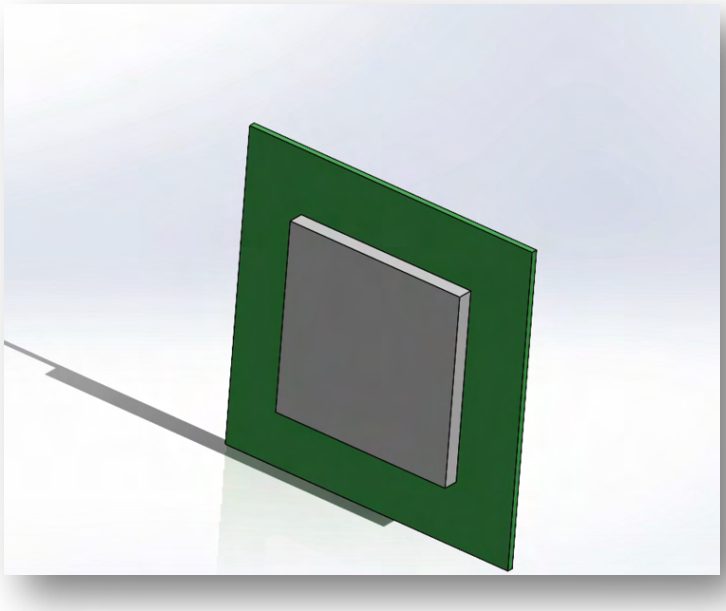

Figure 14 3D Model of Composite with Coating

The Figure 14 above shows the 3D model of the sample for the experimental work. The dimension of the composite slab is 100 X 100 X 2 mm which is shown in green in colour and the coating is 60 x 60 x 5mm which is shown in grey in colour.

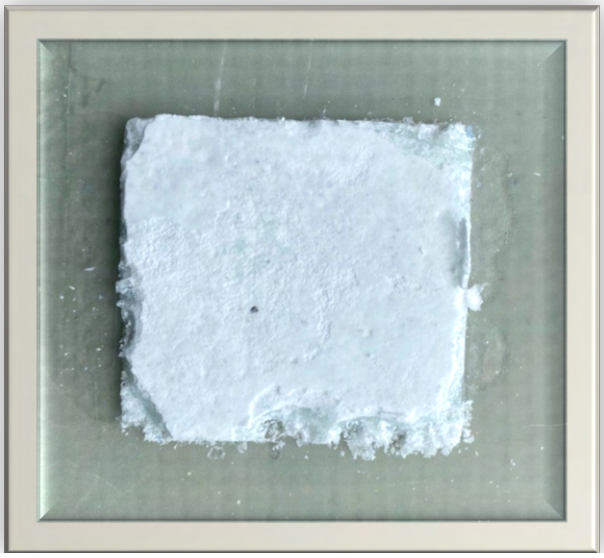

Figure 15 Aerogel Coating on Composite Laminate

Figure 15 shows the case 1 sample which has a coating prepared with 30% volume of RSM 135 epoxy resin and 70% volume of aerogel blend.

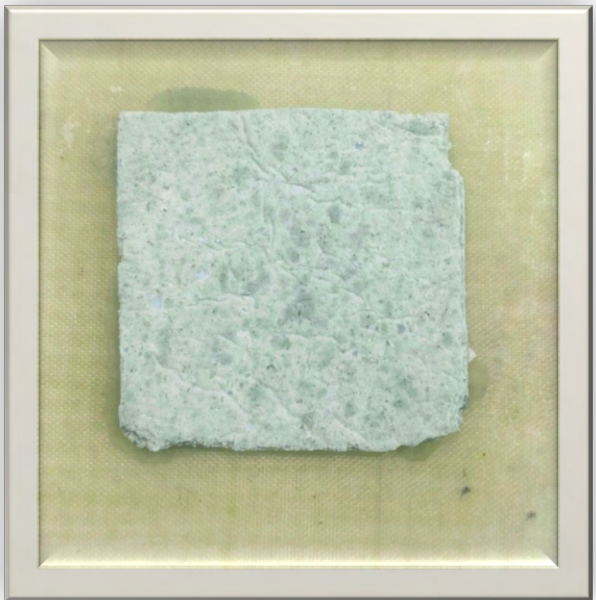

Figure 16 Glass Bubble Coating on Composite Laminate

Figure 16 shows the case 2 sample which has a coating prepared with 30% volume of RSM 135 epoxy resin and 70% volume of glass bubble blend.

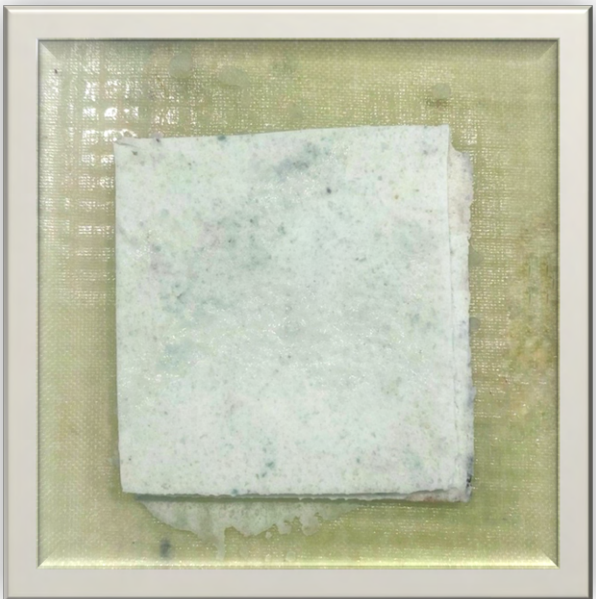

Figure 17 Aerogel and Glass Bubble Blend Coating on Composite Laminate

Figure 17 shows the case 2 sample which has a coating prepared with 30% volume of RSM 135 epoxy resin and 70% volume of glass bubble and aerogel 50:50 blend.

3.4.4 Burn Testing

The composite plate with two different coatings was undergone a flame test as shown in

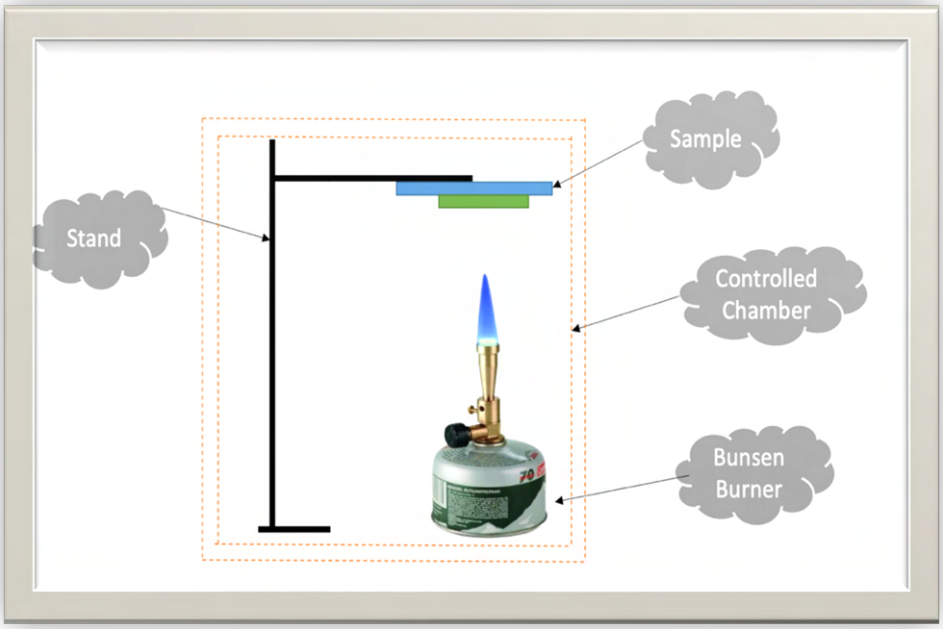

Figure 18 Schematic Representation of Burn Test

In order to test the heat resistance of a sample, it is important to know the temperature of the flame it is exposed to. To determine the flame temperature, a thermocouple can be used. A thermocouple is a device that measures temperature by detecting the voltage produced by a temperature difference between two different metals. In this specific test, the sample is held at a distance of 250mm above the flame, and the temperature of the flame is measured using the thermocouple as shown in Figure 18. The flame temperature is set at 1650°C, which is a very high temperature that is commonly used for testing materials that need to withstand extreme heat.

To ensure consistency and accuracy in the testing process, the sample is held above the flame for a specific amount of time. In this case, the sample is held above the flame for 30 seconds. The time is measured using a stopwatch, which can accurately measure the duration of the test. By conducting this test, it is

possible to determine the heat resistance of the sample. If the sample is able to withstand exposure to the high-temperature flame for 30 seconds without melting, deforming, or catching fire, then it can be considered to have a high level of heat resistance.

4 Results

This section presents the results of the research conducted on high-performance thermal insulation for spacecraft, which aimed to investigate the effectiveness of different insulation materials in reducing heat transfer and maintaining stable temperatures in extreme conditions.
The first set of results presented in this section is the thermal image obtained through lab experimental methods. This image provides a visual representation of the temperature distribution across the insulation material and allows for the identification of any hotspots or areas of uneven heat distribution. The analysis of the thermal image provides valuable insights into the thermal performance of the insulation material and its ability to maintain stable temperatures in extreme conditions.
The second set of results presented in this section are the comparative results from thermal testing conducted in the lab. The thermal investigation involved subjecting the insulation materials to extreme temperatures and measuring their ability to reduce heat transfer. The results of the thermal testing provide quantitative data on the effectiveness of each insulation material in reducing heat transfer and maintaining stable temperatures. The comparative analysis of the results allows for the identification of the most effective insulation material for use in spacecraft.
The third set of results presented in this section is the result of the burn test conducted in the lab. The burn test involved subjecting the insulation materials to high temperatures and measuring their ability to resist burning and maintain their structural integrity. The results of the burn test provide valuable insights into the safety of the insulation materials and their ability to withstand extreme conditions without compromising the integrity of the spacecraft.
Overall, the results of this research suggest that the implementation of high-performance thermal insulation can greatly enhance the efficiency and safety of spacecraft during missions. The comparative analysis of the results presented in this section can inform the selection of the most effective insulation material for use in spacecraft and contribute to the development of more efficient and reliable spacecraft technologies.

4.1 Thermal Image (Lab Experimental Methods)

Detecting defects, delamination, porosity, moisture, deterioration, and microcracking in composites. Composites are anisotropic. Anisotropy and low heat diffusivity in thickness heading restrict recognition of composite defects. The current study introduces a precise technique for recognising damage in composite materials. Uneven and two-sided test strategies were studied. Based on the numerical arrangement of thermal conduction, the perfect mix of thermal motion, heating time, and perception time for 'best thermal insulation detectability'

was determined for each situation, assuming zero commotion. Using these parameter charts as rules, testing was guided, outcomes were compared, and hypothetical forecasts were made. Each cover test's motion attributes were tentatively focused. The same was employed to determine the normal farthest reaches of thermal insulation findings during a test. Polynomial fitting and stage imaging were used to improve contrast and visualise abnormalities.

shows that the composite is getting heated up uniformly. And shows the composite and coating

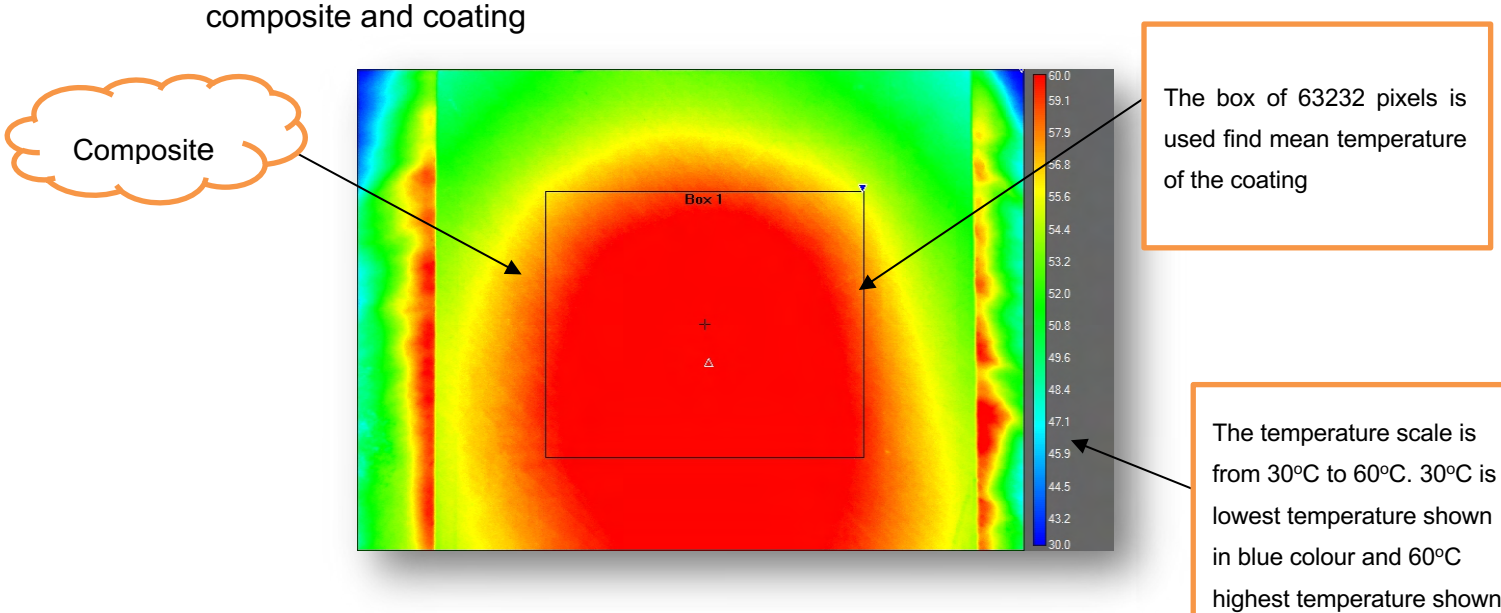

Figure 20 Thermal Image of Composite @ 60C

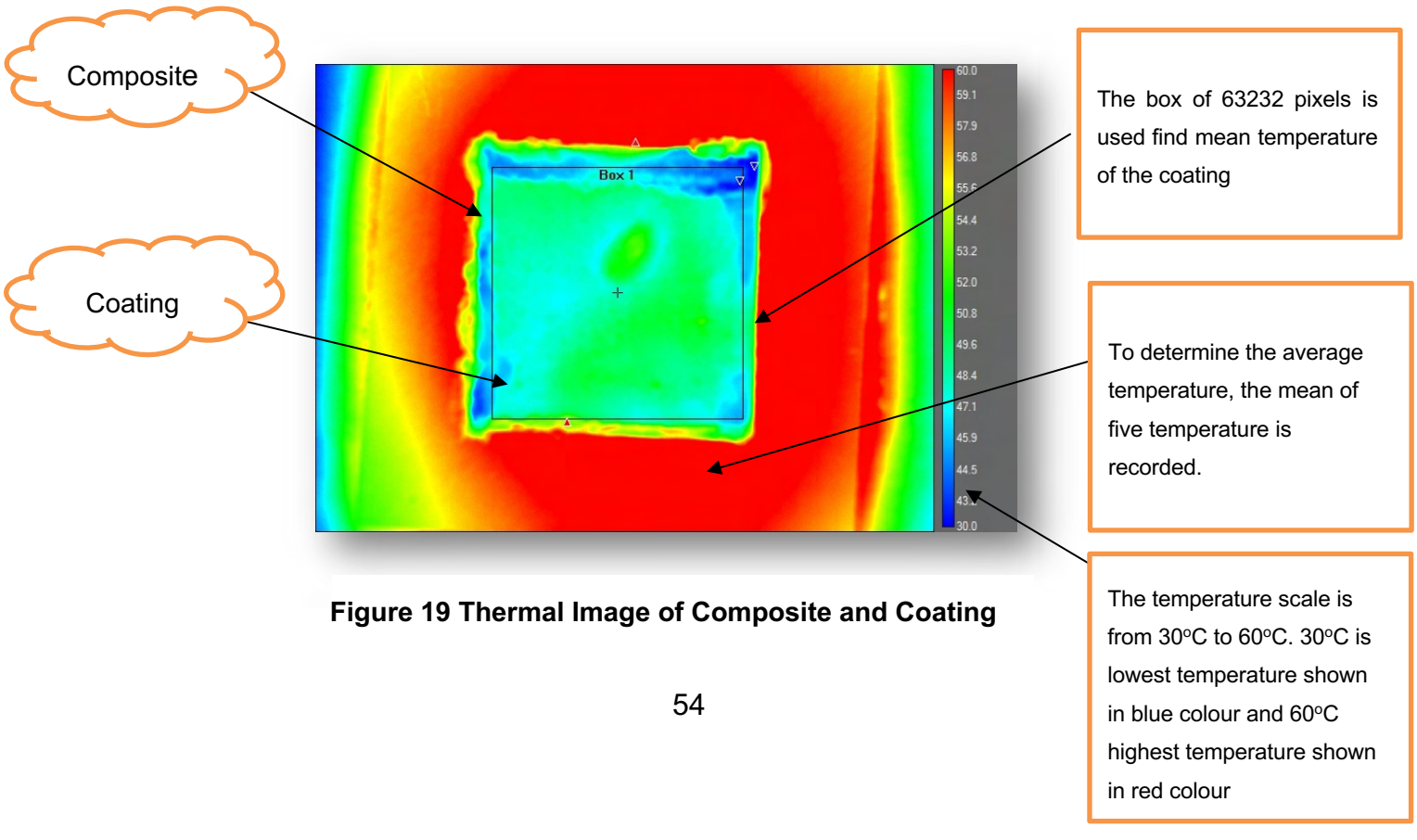

Figure 19 Thermal Image of Composite and Coating

The mean of five temperature is recorded as 44.64°C

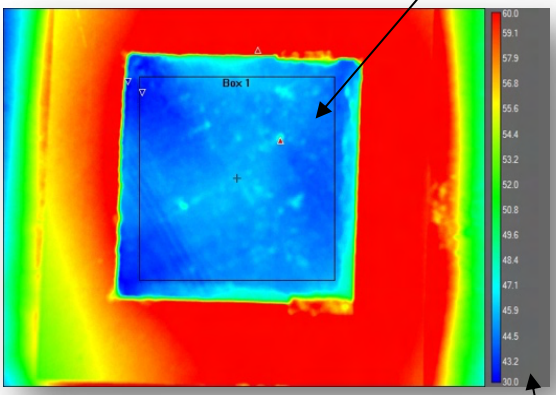

The temperature scale is from 30°C to 60°C. 30°C is lowest temperature shown in blue colour and 60°C highest temperature shown in red colour

Figure 22 Thermal Image of Glass Bubble Coating

The mean of five temperature is recorded as 42.34°C

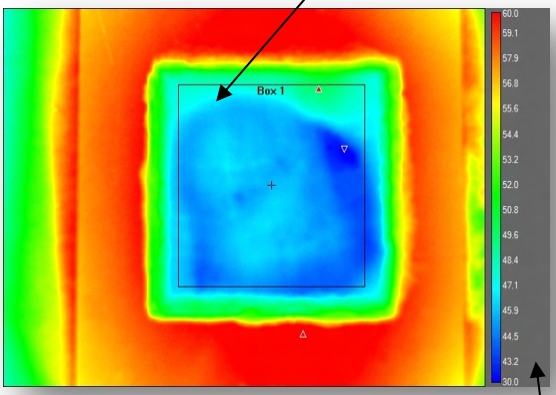

The temperature scale is from 30°C to 60°C. 30°C is lowest temperature shown in blue colour and 60°C highest temperature shown in red colour

Figure 21 Thermal Image of Glass bubble and Aerogel Blend Coating

The mean of five temperature is recorded as 36.45°C

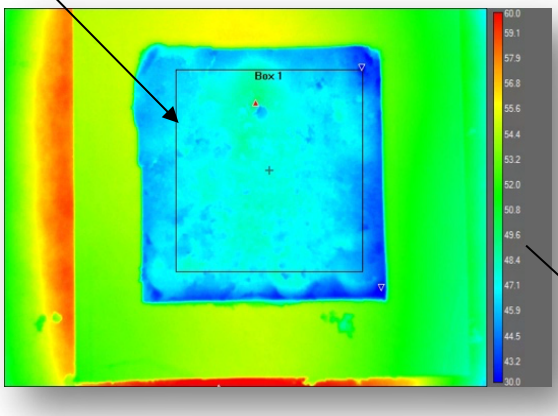

The temperature scale is from 30°C to 60°C. 30°C is lowest temperature shown in blue colour and 60°C highest temperature shown in red colour

Figure 23 Thermal Image of Aerogel Coating

Figure 22 shows the thermal image of the 5mm Glass Bubble coating on composite at 60°C. From the image, it is visible the maximum temperature of the coating reaches 44.64 °C. Figure 21 shows the thermal image of the 5mm Glass Bubble and Aerogel coating on composite at 60°C. From the image, it is visible the maximum temperature of the coating reaches 42.34 °C. Figure 23 shows the thermal image of the 5mm Aerogel coating on composite at 60°C. From the image, it is visible the maximum temperature of the coating reaches 36.45 °C. From the experiments, it is clearly understood that the aerogel epoxy coating insulates the composite better than other coatings.

4.2 Comparative Results from Thermal Testing (Lab Experimental Methods)

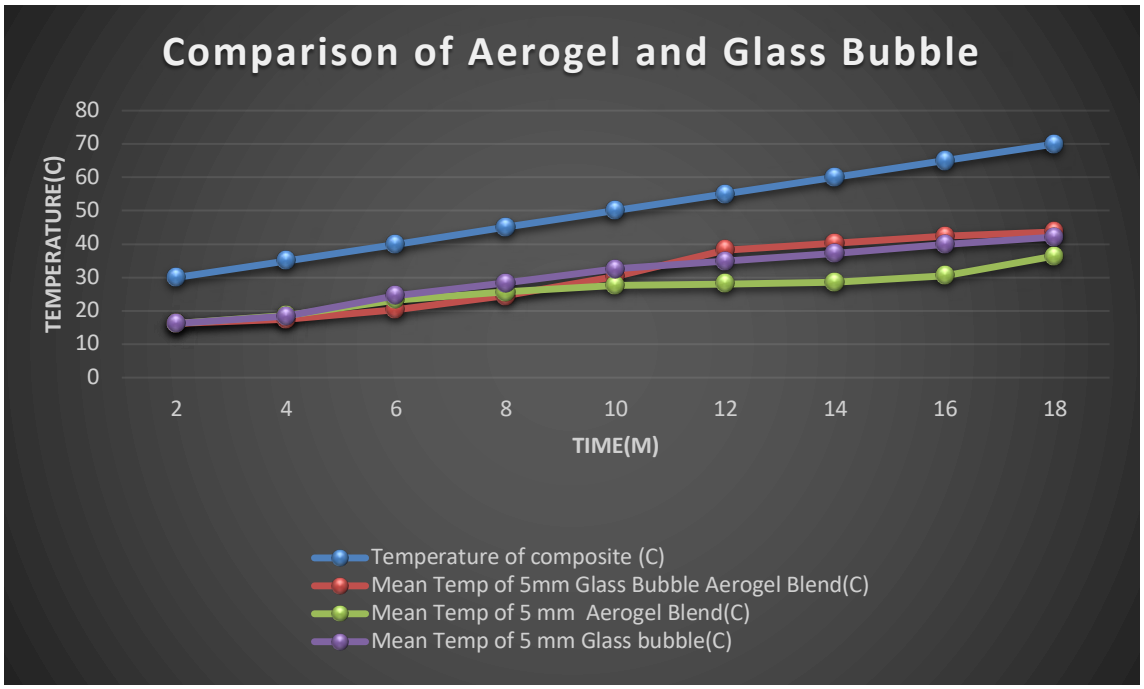

Figure 24 Comparison Graph of Aerogel and Glass Bubble

The Figure 24 above shows the difference in temperature of the coating when aerogel and glass bubble on cured composite. From the above graph, we can see that aerogel gives better insulation when compared to glass bubbles. The reading was taken at different intervals of time using a stopwatch. The

comparison provided is with the use of a coating thickness that is the same throughout (5 mm). The thickness of the coating on Glass Bubble Aerogel is also 5 mm, as is the thickness of the Glass Bubble itself and the coating on the Aerogel.

The graph makes it very evident that aerogel provides superior insulation when compared to alternative coatings. The temperature of the composite with a coating of Glass Bubble Aerogel measuring 5 millimetres is more than 40 degrees Celsius, but the temperature of the composite with a coating of aerogel measuring 5 millimetres is lower than 37 degrees Celsius. Therefore, the minimum thickness of the coating that is required for lowering the inside temperature of the composite to 37 degrees Celsius is between 8 and 10 millimetres with glass bubble aerogel, whereas with aerogel, the thickness needs to be reduced to 4 millimetres in order to achieve the required inside temperature.

4.3 Results of Burn Test (Lab Experimental Methods)

The results of the temperature measurements for the composites coated with aerogel and glass bubble aerogel blend coatings are presented here. The composite coated with the aerogel coating exhibited a composite surface temperature of 230°C. On the other hand, the composite coated with the glass bubble aerogel blend coating showed a higher composite surface temperature of 560°C. These results indicate that the glass bubble aerogel blend coating provides better thermal insulation than the aerogel coating for the composite material. Therefore, the glass bubble aerogel blend coating may be more suitable for applications where high-temperature insulation is required.

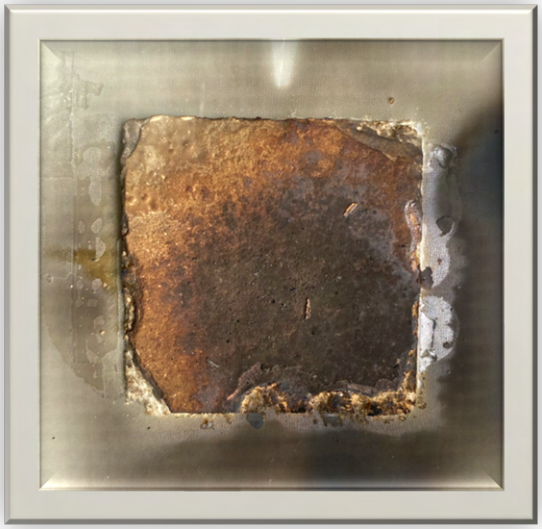

Figure 26 Image of Composite Laminate with Aerogel and Glass Bubble Blend After Burn Test

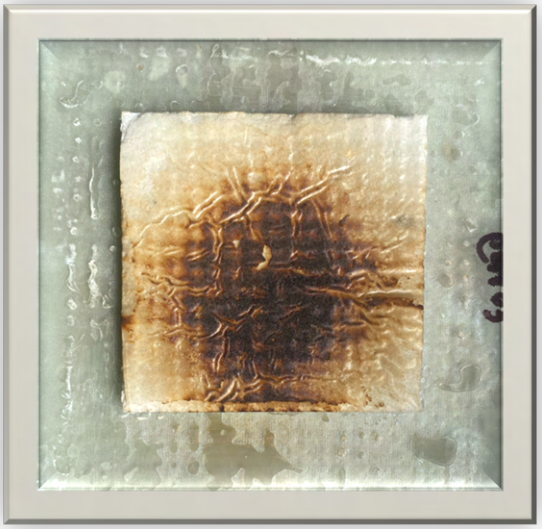

Figure 25 Image of Composite Laminate with Aerogel Coating After Burn Test

The image of the sample after burning is a relevant aspect of this research, as it provides a visual representation of the material's response to heat exposure. The burn test is a common method used to identify the composition of a material, and the image of the sample after burning can help to confirm the results of the test.

In the result section of a thesis, it is important to include the image of the sample after burning, as it provides valuable information about the material's properties. For example, if the material shows signs of melting, deformation, or charring, this may indicate that it is not suitable for use in high-temperature applications. On the other hand, if the material remains intact and does not show any signs of damage, this may indicate that it has good heat resistance properties.

Furthermore, the image of the sample after burning can also provide insights into the effectiveness of the coating material used in this research. The sample coated with the aerogel blend coating Figure 25 shows less damage after burning than the glass bubble aerogel blend sample Figure 26, this would suggest that the coating has helped to improve the heat resistance properties of the material.

5 Discussion

The discussion section of a thesis is a crucial part of the research, as it provides an opportunity to interpret and analyse the results in the context of the research question and the existing literature. In this section, the researcher should provide a comprehensive evaluation of the research findings, discuss the implications of the results, and provide recommendations for future research.

In the present study, the main objective was to investigate the effectiveness of high performance thermal insulation using aerogel coatings for improving the thermal insulation properties of composite materials. The research involved conducting experiments to measure the temperature of the composites before and after exposure to heat, as well as performing a burn test to identify the composition of the material.

The results of the research showed that the aerogel blend coating was more effective than the glass bubble aerogel coating in improving the thermal insulation properties of the composite material. The composite coated with the glass bubble aerogel blend coating exhibited a higher surface temperature after burn than the composite coated with the aerogel coating. This suggests that the aerogel blend coating provides better insulation against high temperatures Table 8.

Table 8 Percentage Decrease of Temperature

Sample	60C	70C	100C	Average
Aerogel	36.45	38.94	39.1	38.1633333
Glass Bubble	40.12	42.57	45.02	42.57

This section of the thesis reveals that the thermal conductivity analysis shows that the pure epoxy samples have a higher thermal conductivity than the aerogel/epoxy combinations. The temperature range that was covered in this research indicates the percentage drop in thermal insulation values for each coating. The aerogel coating showed an average decrease of 39.25%, while the

glass bubble exhibited an average loss of 30%. The reflectance spectra of the samples used in the study showed the presence of epoxy at the 200–250 nm interval for the aerogel coating, providing evidence for the existence of nano-porous aerogel particles. However, further studies are required to verify the theory that wetting ethanol is responsible for the presence of epoxy at 200 nm in the reflectance spectra of the aerogel coating.

Simulations of the three types of coating showed that, at a steady state, the double coating had the least amount of temperature change compared to the two single coating systems. The selection of the coating system depends on the specific requirements of the application. Using the double coating method in settings where there are cyclic loads is recommended since the steady state can be maintained at an almost constant temperature and any changes would be implemented at a slower pace, resulting in a more pleasant atmosphere for any living creatures that could be present at the time. The two single-coating systems arrived at balance more quickly than the double-coating system.

In this study, we investigated the potential inconsistencies in the adjustment of the epoxy on the surface finish and its packing density, which may contribute to performance heterogeneity in aerogel epoxy-based mixed applications that are still in the early stages of development. The significance of this study is further highlighted by the fact that our approach replicates the actual issues and limits encountered on-site, and collecting unique samples from composite prototypes requires extreme care to prevent even minor mechanical manipulation from affecting the final product's performance. Nonetheless, after employing any other technique on a composite plate, specimens can be obtained for testing.

We found that the mechanical behaviour and epoxy absorption were negatively impacted by the large open porosity, highlighting the critical role of the finishing coat in preventing heat loss by acting as a barrier in the outermost layer. Moreover, an increase in porosity could be linked to a decrease in compressive strength, indicating the importance of considering porosity in the design of these materials. Interestingly, our results suggest that epoxy continues to cure even

after its first hardening has taken place, which may contribute to the observed improvement in adhesive strength.

The study also looked at whether it would be possible to use a new thermal rendering covering made with silica aerogel granules as light aggregates in a very hot climate. Even though this product is still in its early stages of development, it could be used for thermal insulation in the near future because it has low thermal conductivity. This means that less material is needed to meet the same thermal insulation needs.

Overall, our results show how important it is to think carefully about the epoxy adjustment and finishing coat when making aerogel epoxy-based mixed applications. They also show how novel thermal rendering coverings could be used in thermal insulation applications. The following inferences can be made from the data obtained:

- Epoxy-based composites integrating silica aerogel can be obtained to provide thermal insulating render with low thermal conductivity (0.0 W/mK), which reduces the composite's footprint in both newly constructed and retrofitted structures.
- The render formulation showed great fresh-state qualities, such as appropriate workability and uniformity, a low bulk density, and an air content within the limits typically considered (a maximum of about 20%);
- Its low bulk density, lack of visible shrinking, and low values for the remaining mechanical characteristics were confirmed. The low compressive strength shows the necessity for additional mechanical protection; the high flexural strength and dynamic modulus of elasticity indicate the capacity to move with the support.
- In terms of its physical qualities, it had poor performance in its resistance to mechanical properties despite having a relatively low thermal conductivity. However, when assessing performance as a multilayer

system, including a protective finishing layer, such attributes can be enhanced.

- All the studies showed that this formulation helped address two major issues with aerogel-based renders: maintaining the integrity of the aerogel granules and ensuring that they were evenly distributed throughout the paste. To do this, aerogel granules were wetted with ethanol.

Glass and epoxy were used to create aerogel micro bond samples, and the adherence of the aerogel to the fibres was characterised using the micro bond technique. The mechanisms of aerogel adhesion to different fibres were next investigated by performing a battery of post-tests and inspecting the fibres' surfaces.

Retaining the aerogel's pore structure in the silica aerogel mix composite is necessary for making a low-conduction-of-heat material. To keep the pores in the aerogel intact during the drying process, a novel method for preparing the silica aerogel mix composite was created. Epoxy and aerogel powder paste filled the gaps in the aerogel composite, but drying in stages rebuilt the porous structure. depicts the thermal conductivity of the silica aerogel blend as a function of volume fraction, showing a linear decrease in value.

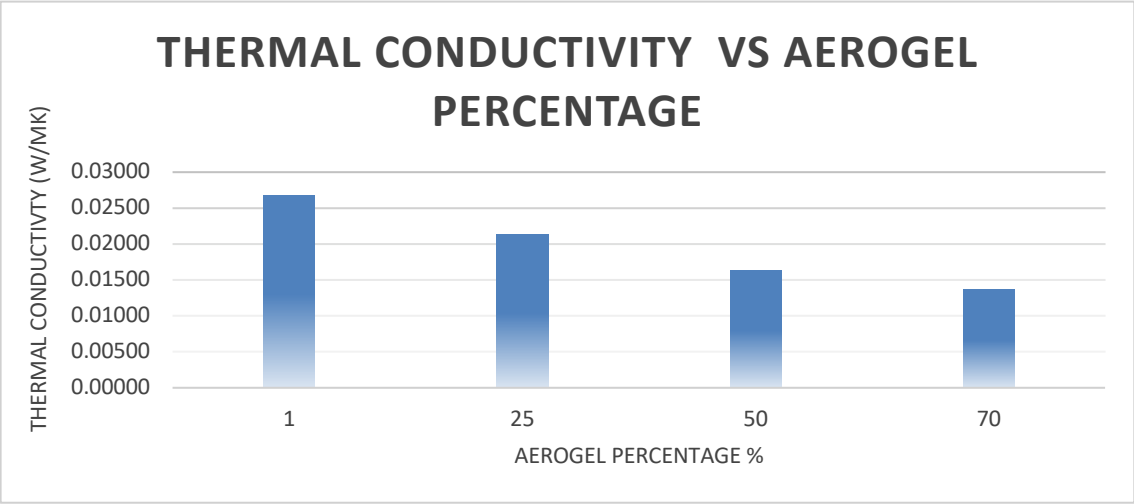

Figure 27 Comparison of Thermal Conductivity with Aerogel Percentage

The Figure 27 above shows the values of thermal conductivity vs aerogel percentage from the theoretical calculation as referred in section 3.1. As the volume fraction of the composites was raised, the thermal conductivity dropped. The lowest value of thermal conductivity for an aerogel composite was found to be 0.0137 W/mK at a volume fraction of 70% aerogel. If this is the case, then aerogel composites should be able to be manufactured with superior insulating qualities compared to other composite coatings.

6 Conclusion And Future Work

This section navigates through conclusion of this entire research and future work.

6.1 Conclusion

Aerogel and epoxy composite coatings on composite substrates for thermal insulation were tested in this study. Aerogel particles with limited resin penetration were detected by the reflectance spectrum and thermal conductivity measurements.

Using a finite element solver, the aerogel coating's performance was modelled and simulated. The coating's performance was affected by the surface in this simulation. Top coating performance was midway between these two metrics. Further research is needed to improve the model, especially using real experimental data as material properties.

The study used composites with glass bubble coating, aerogel coating, and a blend of both. Specifying ambient conditions is necessary to obtain thermal profiles. The research found that the composite with the aerogel coating needs a lower thickness ratio than other coatings to reach the necessary interior temperature of 36.45 degrees Celsius. The aerogel-coated composite has substantially lower deformation and shear ratios than other composites. An aerogel covering can insulate a composite by 40%, protecting spaceship components like electronics.

After that, three case studies calculated fuel and weight savings. In the appendix, it was found that putting an aerogel covering on a composite reduces weight and resource use.

By reducing the spacecraft's bulk and fuel usage, you may save money and ensure its long-term viability. Lowering prices can help crafts become economically viable. If insulated with aerogel, a spaceship can run sustainably, according to the research.

6.2 Future Work

The next potential level of development for this study might include the creation of a true scale model and the subsequent analysis of it with all of the relevant environmental variables. Structures that are more complicated may be evaluated to acquire a more accurate picture of weight and fuel-saving ratios. On the other hand, a real-life version of the toy may be fabricated using composite material and an aerogel coating of varying thickness, and it can be evaluated in an environmental chamber at a research facility. In the future, research could uncover an alternative coating that is superior to aerogels. In the future, it will be possible to conduct damage characterization of the composite with an aerogel coating, which will assist in locating the material's deterioration. In addition, we are able to evaluate the mechanical performance of the aerogel coating by a variety of tests, such as tensile testing, dynamic testing, and so on. Combining graphene with polymers may result in a considerably more intensive packing density, which can be used to get higher mechanical qualities.

It is possible to do an analysis or use a technique that measures impact energy in order to determine the degree of impact energy that will be experienced while entering and exiting space.

REFERENCES

Aglietti, G. S. (2020). Current Challenges and Opportunities for Space Technologies. *Frontiers in Space Technologies*, *1*(1), 1. https://doi.org/10.3389/frspt.2020.00001

Babels, H. W., Jones3, C., & David$, K. (1996). *DESIGN PROPERTIES FOR STATE-OF-THE-ART THERMAL CONTROL MATERIALS FOR MANNED SPACE VEHICLES IN LEO?* (Vol. 39, Issue 5).

Barrios, M., & Van Sciver, S. W. (2010). An apparatus to measure thermal conductivity of spray-on foam insulation. *AIP Conference Proceedings*, *1218*, 938–945. https://doi.org/10.1063/1.3422463

Brindza, P., Sun, E., Lassiter, S., & Fowler, M. (2010). Cryostat design and analysis of the superconducting magnets for Jefferson Lab's 11 GeV/c super high momentum spectrometer. *AIP Conference Proceedings*, *1218*, 957–964. https://doi.org/10.1063/1.3422465

Congdon, E. A., Mehoke, D. S., Buchta, M., Nagle, D., Zhang, D., & Spicer, J. B. (2010). Development of a high-temperature optical coating for thermal management on solar probe plus. *10th AIAA/ASME Joint Thermophysics and Heat Transfer Conference*, *July*, 1–9. https://doi.org/10.2514/6.2010-4661

Cornaro, C., & Buratti, C. (2020). Energy efficiency in buildings and innovative materials for building construction. *Applied Sciences (Switzerland)*, *10*(8). https://doi.org/10.3390/APP10082866

Debnath, B., Shakur, M. S., Tanjum, F., Rahman, M. A., & Adnan, Z. H. (2022). Impact of Additive Manufacturing on the Supply Chain of Aerospace Spare Parts Industry—A Review. *Logistics*, *6*(2), 28. https://doi.org/10.3390/LOGISTICS6020028

del Val, A., Luís, D., & Chazot, O. (2022). Experimental methodology for the accurate stochastic calibration of catalytic recombination affecting reusable

spacecraft TPS. *Chemical Physics*, *559*(February), 111528. https://doi.org/10.1016/j.chemphys.2022.111528

Dombrovsky, L. A., Reviznikov, D. L., Kryukov, A. P., & Levashov, V. Y. (2017). Self-generated clouds of micron-sized particles as a promising way of a Solar Probe shielding from intense thermal radiation of the Sun. *Journal of Quantitative Spectroscopy and Radiative Transfer*, *200*, 234–243. https://doi.org/10.1016/j.jqsrt.2017.06.025

Dye, S., Kopelove, A., & Mills, G. L. (2010). INTEGRATED AND LOAD RESPONSIVE MULTILAYER INSULATION. *AIP Conference Proceedings*, *1218*(1), 946. https://doi.org/10.1063/1.3422464

Gogu, C., Bapanapalli, S. K., Haftka, R. T., & Sankar, B. V. (2009). Comparison of materials for an integrated thermal protection system for spacecraft reentry. *Journal of Spacecraft and Rockets*, *46*(3), 501–513. https://doi.org/10.2514/1.35669

Goodhew, P. J., Clarke, A. J., & Bailey, J. E. (1975). A review of the fabrication and properties of carbon fibres. *Materials Science and Engineering*, *17*(1), 3–30. https://doi.org/10.1016/0025-5416(75)90026-9

Gordon, T., Xu, X., Wisnom, M. R., Hallett, S. R., & Chul Kim, B. (2023). Improved impact damage resistance of tapered composite laminates using a ply scarfing technique. *Composites Part A: Applied Science and Manufacturing*, *166*. https://doi.org/10.1016/j.compositesa.2022.107391

Gurav, J. L., Jung, I. K., Park, H. H., Kang, E. S., & Nadargi, D. Y. (2010). Silica aerogel. *Journal of Nanomaterials*, *2010*, 11. https://doi.org/10.1155/2010/409310

Johnson, J. A., Heidenreich, J. J., Mantz, R. A., Baker, P. M., & Donley, M. S. (2003). A multiple-scattering model analysis of zinc oxide pigment for spacecraft thermal control coatings. *Progress in Organic Coatings*, *47*(3–4), 432–442. https://doi.org/10.1016/S0300-9440(03)00133-4

Keesee, C. J. E. (n.d.). *Spacecraft Thermal Control Systems • Purpose of thermal control systems*. 1–40.

Miao, J., Tu, X., Peng, N., & Hou, R. (2022). *Active vibration control of spacecraft solar panel using solid propellant microthruster array*. 222. https://doi.org/10.1117/12.2653103

Miao, J., Zhong, Q., Zhao, Q., & Zhao, X. (2021). *Spacecraft Thermal Control Technologies Space Science and Technologies Series Editor: Peijian Ye*.

Natali, M., Rallini, M., Kenny, J., & Torre, L. (2016). Effect of Wollastonite on the ablation resistance of EPDM based elastomeric heat shielding materials for solid rocket motors. *Polymer Degradation and Stability*, *130*, 47–57. https://doi.org/10.1016/j.polymdegradstab.2016.05.019

Nenarokomov, A. V., Alifanov, O. M., Budnik, S. A., & Netelev, A. V. (2016). Research and development of heat flux sensor for ablative thermal protection of spacecrafts. *International Journal of Heat and Mass Transfer*, *97*, 990–1000. https://doi.org/10.1016/j.ijheatmasstransfer.2016.02.045

Nguyen, S., Anthony, D. B., Qian, H., Yue, C., Singh, A., Bismarck, A., Shaffer, M. S. P., & Greenhalgh, E. S. (2019). Mechanical and physical performance of carbon aerogel reinforced carbon fibre hierarchical composites. *Composites Science and Technology*, *182*(March). https://doi.org/10.1016/j.compscitech.2019.107720

Nicolai', B. M., & De Baerdemaeker, J. (1996). Sensitivity Analysis with Respect to the Surface Heat l'kansfer Coefficient as Applied to Thermal Process Calculations. In *Journal of Food Engineering* (Vol. 28).

Rawal, S. (2018). Materials and structures technology insertion into spacecraft systems: Successes and challenges. *Acta Astronautica*, *146*, 151–160. https://doi.org/10.1016/J.ACTAASTRO.2018.02.046

Reynolds, E., Driesman, A., Kinnison, J., Lockwood, M. K., & Hill, P. (2013). Solar Probe Plus mission overview. *AIAA Guidance, Navigation, and Control (GNC) Conference*, 1–11. https://doi.org/10.2514/6.2013-4879

Shahedan, N. F., Abdullah, M. M. A. B., Mahmed, N., Kusbiantoro, A., Tammas-Williams, S., Li, L. Y., Aziz, I. H., Vizureanu, P., Wysłocki, J. J., Błoch, K., & Nabiałek, M. (2021). Properties of a New Insulation Material Glass Bubble in Geopolymer Concrete. *Materials 2021, Vol. 14, Page 809*, *14*(4), 809. https://doi.org/10.3390/MA14040809

Shen, X., Jiao, T., Zhang, Q., Guo, H., Lv, Y., Zhou, J., & Gao, F. (2013). Nanostructures and self-assembly of organogels via benzimidazole/ benzothiazole imide derivatives with different alkyl substituent Chains. *Journal of Nanomaterials*, *2013*. https://doi.org/10.1155/2013/409087

Universités, P., Paris, U., Sorbonne, D., & Cité, P. (1987). *Jean-Louis Adrien Thèmes de recherche Recherches en cours Principales publications*. 2–4. https://doi.org/10.1155/2010

Uyanna, O., & Najafi, H. (2020). Thermal protection systems for space vehicles: A review on technology development, current challenges and future prospects. *Acta Astronautica*, *176*(June), 341–356. https://doi.org/10.1016/j.actaastro.2020.06.047

Yum, S. H., Kim, S. H., Lee, W. Il, & Kim, H. (2015). Improvement of ablation resistance of phenolic composites reinforced with low concentrations of carbon nanotubes. *Composites Science and Technology*, *121*, 16–24. https://doi.org/10.1016/j.compscitech.2015.10.016

Zhang, J., Chevali, V. S., Wang, H., & Wang, C. H. (2020). Current status of carbon fibre and carbon fibre composites recycling. *Composites Part B: Engineering*, *193*(December 2019), 108053. https://doi.org/10.1016/j.compositesb.2020.108053

Zhang, Y., Sarvey, T. E., & Bakir, M. S. (2017). Thermal Evaluation of 2.5-D Integration Using Bridge-Chip Technology: Challenges and Opportunities. *IEEE Transactions on Components, Packaging and Manufacturing Technology*, *7*(7), 1101–1110. https://doi.org/10.1109/TCPMT.2017.2710042

APPENDICES

Appendix A

A.1 THE PRESENT PROBLEMS ENCOUNTERED BY SPACECRAFT

The following is a list of the five most common obstacles that spacecraft must overcome:

1. **Propulsion System**

The effective operation of propulsion systems is also essential to the completion of interplanetary missions since it enables faster travel and the transportation of larger payloads to the desired destinations. Our current limitations in the monitored examination of the local planetary group are mostly the result of the duration of travel, which is directly related to the level of performance that is available from our existing propulsion system. As a result, the operation of our propulsion system places limitations on our capabilities for research and abuse (in addition to those for mechanical workouts), as it is a significant limitation on the amount of payload mass that can be transported safely to and from other divine bodies(Brünner et al., 2018). As shown in Figure Apx A 1

Figure Apx A 1 Propulsion System

2. Protection of Humans

Human exploration includes the study of space health and medicine (Hodkinson et al., 2017), with the goal of enabling people to survive the space environment for extended periods of time, as well as the creation of artificial environments in space and on other planets, with the goal of facilitating a natural form of human life. The purpose of this experiment is to see if it is possible to create an entirely fictitious environment that is beneficial to people's prosperity as well as their physical and emotional well-being, while also providing protection against the potentially detrimental effects of the space environment (Grimm, 2019). Whether we are considering a man-made vessel for considerable distance space travel, a space stage for large-scale human inhabitation, or a planetary settlement, there are a few challenges that are universal. These encompassing challenges include the requirement to develop efficient closed-loop systems for the replenishment of resources and the reduction of waste, with the overarching goal of developing a synthetic biological system for the extended support of human existence(Brünner et al., 2018).

3. Earth Environment

To continue with the theme of the protection of the Earth, environmental change poses a significant threat to our condition, one that might have catastrophic effects; this is an area in which satellite technologies can assist in the management of the challenge (Brünner et al., 2018). Satellites provide objective data on a global scale, which may be used to monitor the globe, develop models of it, and get those models approved. This helps improve our ability to predict the future. In any event, a more significant amount of effort needs to be made into developing important data that is identified with specific requirements and issues. This will help reduce the enormous amount of information to fewer difficult translations that can guide political discourse(Brünner et al., 2018).

4. Low-Cost Space Technologies

Other specialised constraints, such as the requirement to achieve high stage solidity, affect all smaller mass satellites, not just CubeSats, and provide

significant challenges. This includes the fact that these issues are not unique to CubeSats. This is important for all missions that support optical payloads that are extremely precisely focused (for example, high-goal cameras/telescopes or laser communication systems) or for devices that require protection for inertial types of estimations. The issue lies with the minimization of the smaller scale vibrations that are produced by fundamental on-board hardware and that can, for example, induce improper motions of the view. The solution lies in the minimization of these smaller scale vibrations. This problem is particularly severe for more diminutive specialties since there is less mass (dormancy), which would ordinarily lower the intensity of vibration. Ground testing and exhibiting to anticipate in-circle performance are still not accurate, and the utilisation of enormous edges rather than exact models is required for successful application development. At the lower end of the market, where the majority of development is usual, dynamic control of miniaturised scale vibrations is still difficult and too expensive to possibly be actualized. This is especially true at the lower end of the market. CubeSat capacities are frequently oversold to an unpractised audience, and there is a general demand for better products with the included equipment that nevertheless maintains reasonable prices. This is because there is a general necessity for better products with the included equipment(Brünner et al., 2018).

5. Large Space Structures

The ability to transport LSS is a further factor that, in a manner similar to that of propels in impetus, would enable a variety of purposes; nonetheless, they provide a series of significant challenges, the nature of which varies depending on the locations. From one point of view, there are devices such as telescopes, cameras, and reception apparatuses that require a huge (more than ten metres and possibly a significant amount larger) high-precision intelligent surface. In this context, the current systems (e.g., based on the arrangement of completely machined and cleaned mirrors whose positions and shape can be balanced by a progression of actuators) are constrained by the size and number of sections that can be transported [for example, the James Webb Space Telescope (JWST)4], as well as the overall staggering cost. Concerning the radio lines, a variety of deployable arrangements have been suggested. These arrangements range

from inflatables to tensegrity structures. However, Europe still has to develop a suitable business response for both current and future applications. In general, new innovations that are smaller in weight need to be delivered in order to expand packaging proficiency without compromising the quality of the previous reflector(Brünner et al., 2018).

A.2 WEIGHT CALCULATION ON 3D SLAB MODEL

Figure Apx A 2 depicts the three-dimensional slab model that was utilised for the study, and the calculations for conserving weight are as follows.

Composite material with a ceramic coating (3D Slab) priced per square metre

A metre is equal to one thousand millimetres.

One metre is equal to one thousand millimetres.

Height equals 100 millimetres or 0.1 metres.

We are aware that the formula for calculating density is as follows: Density = mass divided by volume

Hence The equation for mass is density multiplied by volume.

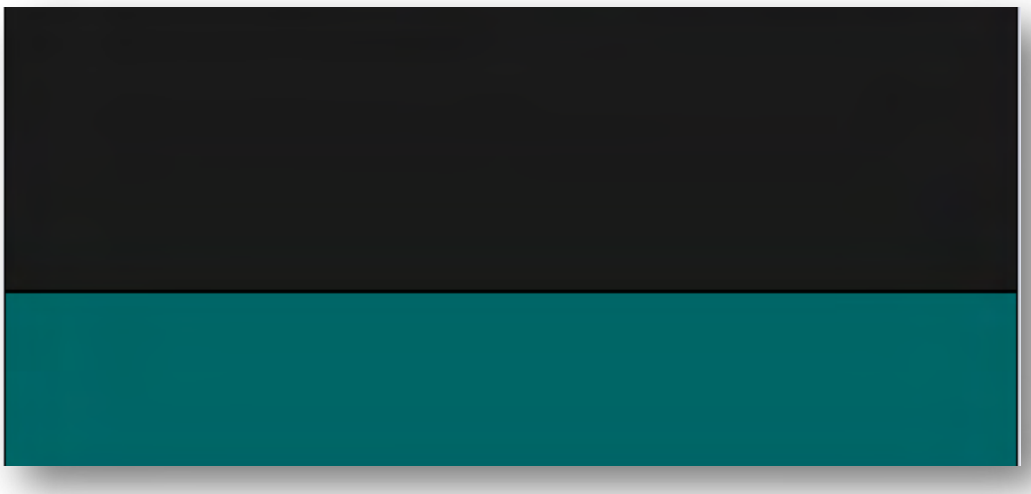

Figure Apx A 2 3D Slab Model

Therefore, the volume of the three-dimensional slab per square metre when utilising ceramic insulation is equal to the length times the width times the height, which equals 1 * 1 * 0.1.

Volume = 0.1m3

Ceramic has a density equal to 3900 kg/m3.

Mass = 3900 * 0.1= 390Kg

Total mass = 390 Kg

Composite material with an aerogel coating (3D Slab) priced per square metre

A metre is equal to one thousand millimetres.

One metre is equal to one thousand millimetres.

Height = 4 mm=0.004m

We are aware that the formula for calculating density is as follows: Density = mass divided by volume

Hence The equation for mass is density multiplied by volume.

Therefore, the volume of the three-dimensional slab per square metre when utilising ceramic insulation is equal to the length times the width times the height. The formula for height is: 1 * 1 * 0.1

Volume = 0.004m3

Ceramic has a density equal to 80 kg/m3

Mass = 80 * 0.004= 0.32Kg

Total mass = 0.32 Kg

The calculation indicates that the overall weight of the ceramic coating is 390 kilogrammes, whereas the total weight of the aerogel coating is 0.32 kilogrammes.

Because of this, the total amount of weight that might be saved per square metre by applying an aerogel coating is 389.68 kilogrammes per square metre.

A.3 CALCULATION OF WEIGHT REDUCTION AND FUEL SAVINGS FOR THREE CASES

- **Nose Tip**

Figure Apx A 3 Nose Tip

Figure Apx A 3 is the tip of a rocket and has the following dimensions:

1.91 m in height (1911 mm)

The diameter is 1080 millimetres or 1.08 metres.

Circumference: 540 mm (0.54 m)

The tip of the nose's surface area is equal to * r (r + (h2+r2)).

= 3.14, r = nose tip radius

A person's nose's height is denoted by the symbol h.

The formula for the surface area is: A = 3.14*0.54 (0.54 + (1.912+0.542)).

= 4.28 m^2

The ceramic-coated nose tip has a mass of 1669.2 kg.

The aerogel-coated nose weighs in at a hefty 1.36 kg.

A total of 1667.8 Kg may be cut if the nose tip is coated with aerogel.

One kilo of payload takes six kilos of propellant, so we can avoid wasting the approximate one hundred and oh-six thousand kilogrammes of fuel.

In this scenario, aerogel coating the nose may lower its weight, which in turn saves fuel.

- **Body Tube of Atlantis Space Shuttle**

Figure Apx A 4 Body Tube of Atlantis

Figure Apx A 4 and its proportions are as follows, the Atlantean body tube is:

Those who measure their height in millimetres will find that 20.1 m Equals 20,100 mm.

8.7 m in diameter (or 8700 mm)

This means that a radius of 4.35 metres requires a diameter of 4350 mm.

The formula for the area of a body tube is $2\pi rh + 2\pi r^2$

where r is the radius of the tube.

h = tube body height

As a result, surface area equals $2^* 3.14^* 4.35^* 20.1 + 2 *3.14^* (4.35)^2$

$= 664.1\ m^2$

The nose tip with ceramic coating has a weight of 25.9013 Kg.

With aerogel coating, the nose tip is 212.5 Kg.

If the body tube is coated with aerogel, we can save a total of 258,800.5 kg.

In this situation, the 1552.8*103 kg (approx.) of fuel may be spared since it takes 6kg of propellant to launch 1kg of payload.

In this scenario, aerogel coating the body tube may decrease its overall mass, which in turn results in lower fuel consumption.

- **Heat shielding section for astronauts to bring from space to earth**

Figure Apx A 5 Heat Shield

Figure Apx A 5 is the heat shield that has the following dimensions:

Height = 2250 mm = 2.25 m

Diameter = 2430 mm = 2.43 m

Radius = 1215 mm = 1.215 m

Area of heat shield = = π * r (r + $\sqrt{h^2 + r^2}$)

Π = 3.14

r = the heat shield's diameter

h = the heat shield's height

So, the area is 3.14* 1.215 (1.215 + $\sqrt{2.25^2 + 1.215^2}$) =14.39 m2

The ceramic coating on the heat shield makes it weigh 5612.45 kg.

4.60 Kg is the weight of the heat shield with an aerogel coating.

5607.85 Kg of weight can be saved if the heat shield is coated with aerogel.

It takes 6 kg of fuel to launch 1 kg of payload, so the 33647 kg (approximately) of fuel can be saved in this case.

In this case study, the heat shield can be made lighter and save fuel if it is coated with aerogel.

In all of these situations, if aerogel coating is used, the spacecraft can be made lighter and use less fuel, which can lower the overall cost of the spacecraft.